ISTANBUL TECHNICAL UNIVERSITY ★ INFORMATICS INSTITUTE

**DESIGN OF A NEW
ULTRA WIDEBAND (UWB) MICROSTRIP ANTENNA**

M.Sc. THESIS

Vala TASHVIGH

Department of Communication Systems

Satellite Communication and Remote Sensing Programme

Thesis Advisor: Prof. Dr. M. Tayfun GÜNEL

JANUARY 2015

ISTANBUL TECHNICAL UNIVERSITY ★ INFORMATICS INSTITUTE

**DESIGN OF A NEW
ULTRA WIDEBAND (UWB) MICROSTRIP ANTENNA**

M.Sc. THESIS

Vala TASHVIGH
(705111025)

Department of Communication Systems

Satellite Communication and Remote Sensing Programme

Thesis Advisor: Prof. Dr. M. Tayfun GÜNEL

JANUARY 2015

İSTANBUL TEKNİK ÜNİVERSİTESİ ★ BİLİŞİM ENSTİTÜSÜ

**YENİ BİR ULTRA GENİŞ
BANDLI MİKROŞERİT ANTEN TASARIMI**

YÜKSEK LİSANS TEZİ

Vala TASHVIGH
(705111025)

İletişim Sistemleri Anabilim Dalı

Uydu Haberleşmesi ve Uzaktan Algılama Programı

Tez Danışmanı: Prof. Dr.M. Tayfun GÜNEL

OCAK 2015

Vala TASHVIGH, a **M.Sc.** student of ITU Informatics Institute student ID **705111025**, successfully defended the **thesis** entitled "**DESIGN OF A NEW ULTRA WIDEBAND (UWB) MICROSTRIP ANTENNA**", which he prepared after fulfilling the requirements specified in the associated legislations, before the jury whose signatures are below.

Thesis Advisor :   **Prof. Dr. M. Tayfun GÜNEL**   ....
İstanbul Technical University

Jury Members :   **Prof. Dr. Sedef KENT PINAR**   ....
İstanbul Technical University

Prof. Dr. Funda AKLEMAN YAPAR   ....
İstanbul Technical University

Date of Submission : 11 December 2014
Date of Defense :   21 January 2015

To my Parents,

FOREWORD

I would like to express my deepest appreciation and gratitude to my academic and research advisor, Professor. Dr. M. Tayfun GÜNEL for his advice and invaluable guidance throughout my research. This work would have been impossible without his precious support and encouragement. After all my great thanks to my mother, father and specially my sweet heart, which this work was not possible without their supports and I had always felt their prays with me.

x

TABLE OF CONTENTS

ABBREVIATIONS

FCC	:	Federal Communications Commission
UWB	:	Ultra WideBand
HFSS	:	High Frequency Structural Simulator
PICA	:	Planar Inverted Cone Antenna
PIFA	:	Planar Inverted F Antennas
DGS	:	Defected Ground Structure
EIRP	:	Effective Isotropic Radiated Power
MB-OFDM	:	MultiBand Orthogonal Frequency Division Multiplexing
IR-UWB	:	Impulse Radio-Ultra WideBand
BW	:	BandWidth
PPM	:	Pulse Position Modulation
PAM	:	Pulse Amplitude Modulation
OOK	:	On-Off Keying
BPSK	:	Binary Phase Shift Keying
WUSB	:	Wireless Universal Serial Bus
Wi-Media	:	Wireless Media
GBR	:	Ground Penetrating Radar
WLAN	:	Wireless Local Area Network
PAN	:	Personal Area Network
RFID	:	Radio Frequency Identification
ITU-R	:	International Telecommunication Union-Radio communication
RBW	:	Resolution Band Width
PRF	:	Pulse Repetition Frequency
RF	:	Radio Frequency
IEEE	:	Institute of Electrical and Electronics Engineers
RADAR	:	Radio Detection And Ranging
VSWR	:	Voltage Standing Wave Ratio
VNR	:	Vector Network Analyser
MATLAB	:	Matrix Laboratory
CST	:	Computer Simulation Technology
FEM	:	Finite Element Method

LIST OF TABLES

LIST OF FIGURES

DESIGN OF A NEW ULTRA WIDEBAND (UWB) MICROSTRIP ANTENNA

SUMMARY

Demands for high rate and broad band communication technologies have been increased in recent years. These requirements lead organization such as FCC to define a new frequency range and standards to fulfill the needs. One of these standards today known as Ultra Wideband (UWB). The following thesis focused on this technology and tried to present a practical design of antenna supporting UWB systems.

UWB technology is clearly presented in the second chapter and explains different approaches used to cover its requirements. The technology itself, without its implementation would be meaningless; therefore, methods of implementation and main applications of this technology will be described briefly.

Methods of implementing UWB technology on microstrip substrate antenna disscussed in chapter three. A short introduction about the history of antennas will be good start for this chapter. The key to understand an antenna and its functioning is electromagnetic radiation.

Despite prevalent believes, there is no need to be specialist in integro-differential equations to understand electromagnetic radiation. In order to grasp the concepts of electromagnetic radiation, one only needs to understand the electricity and magnetism. Researches in these fields, goes back to nearly two thousand years. Great scientists worked in these fields to deliver the great results to James Clerk Maxwell, who is the most known person in electromagnetic fields for what are currently called the Maxwell equations.

In this chapter, it's tried to cover all the materials might be required for design procedure. Different feeding techniques that are used in microstrip antennas are also described. Last part of chapter three presents different techniques for widening the bandwidth.

In chapter 4, a new heptagon shape microstrip antenna is presented. The antenna is fed using probe feeding technique with uniform ground plane. Proper slots have been employed to enhance the bandwidth. The antenna is designed and fabricated on the substrate of FR4 which will decreases the cost of fabrication as an important factor in industry. All the simulations have been done using HFSS software.

YENİ BİR ULTRA GENİŞ BANDLI MİKROŞERİT ANTEN TASARIMI

ÖZET

Antenleri dikkate almadan kablosuz teknolojilerden konuşmak boşuna olur. İyi ve güvenilir kablosuz bağlantı yeterli iletim gücü, yeterli bant genişliği vs gerektirir. Bu şartları sağlamak amacıyla sistemin her parçası iyi çalışmalıdır, Ve anten bir sistemin başlangıç veya son kısmı olarak önemli bir rol oynar. Son yıllarda mikroşerit teknolojilerin getirilmesiyle mikroşerit antenler sanayi ve akademik çevrelerde ilgi odağı haline geldi. Teknolojideki bu gelişmelerin arasında bileşenlerin küçültülmesi, daha fazla bilgi iletmek için daha fazla bant genişliği sağlamak sayılabilir. Öte yandan anten talepler frekans bantları doygunluğuna yol açtı. Dolayısıyla teknolojinin bu sorunların üstesinden gelmek için bir başka devrime ihtiyaç duyuyordu.

Ultra geniş band (UWB), bu yukarıda bahsedilen sorunların üstesinden gelmek için getirilen bu devrimsel teknolojilerden biri dir. Sorunları 3.1 ila 10.6 GHz arası kullanılan bantları tekrar ancak bu sefer daha düşük güç iletimi üzerinden kullanmak suretiyle çözmeye çalışmaktadır. Düşük iletim gücü kullanan bu teknik bu yolla diğer dar bantlı telsiz/radyo sistemlerini için görünmez hale gelmekte ve kullanılan spektrumun paylaşılmasına olanak vermektedir. Cihazların oldukça düşük güç altında çalışabilme kapasitesi ile birlikte yeterince hızlı çalışması gerektiğinden UWB teknolojilerini uygulamanın oldukça karmaşık olduğu da dikkatlerden kaçmamalıdır. Dolayısıyla bu sistemlerdeki antenlerin düşük bir güç altında sinyal alıp-gönderme kabiliyeti ile birlikte ultra geniş bant yelpazesinde çalışması gerekmektedir.

Bu tezde UWB uygulamaları için bir mikroşerit anten geliştirilmiştir. Bugünün yaşam tarzında cihazların büyüklüğü önemli bir husus oluşturuyor. Dolayısıyla Çoğu UWB uygulamalarını kapsamak için bant genişliğini sabit tutulurken boyutları küçültmek için çalışmalar yapılmaktadır. Üretim masrafları önemli bir rol oynadığından antenler FR4 alt katmanlarında tasarlanıp imal edilmiştir.

Bu çalışmada önerilen antenin boyutunu halen UWB frekans bant aralığını sağlayarak düşürmek için örneğin uygun yama biçimi kullanmak ve yarık uygulamak gibi farklı yöntemler denenmiştir.

Son yıllarda yapılan çalışmalara bakıldığında daha büyük bant genişliğine ulaşmak için çok-katmanlı anten kavramı ilk kez Hall ve diğerleri [1] tarafından ortaya atıldı. Standart bir yama antenden 16 kat daha geniş bant genişliği sağlayan bu antenler artırılmış yüksekliğe sahip alüminyum alt katmanlardan imal edilmiştir. C. Wood tarafından ortaya atılan bir diğer yöntem. Mikro-şerit yama antenlerin bant genişliğini ikiye katlamaktadır [2].

Demeryd ve Karlsson [3] düşük yalıtkanlık sabitli daha kalın katmanlar kullanarak geniş bantlı bir mikroşerit anten tasarladı. Bu anten geniş bant için bir dizi içerisinde bir anten elemanı olarak kullanıldı. Dairesel yama antenin bir temel geniş bant anten olduğunu varsayarak N.Das ve Chateljee [4] çok daha geniş bant genişliğine sahip konik bir mikro-şerit anten geliştirdi. Bu antenin tasarımı, dairesel yama antenin yama yapısını katman içine hafifçe konik olarak bastırmak suretiyle değiştirilmesine dayalıdır.

Sabban [5], %15 bant genişliği artışıyla bir 64-elemanlı Ku bant diziliminin baz elemanı olarak iki katmanlı ikiz anten geliştirdi. Bhatnagar ve diğerleri [6] bant genişliğini artırmak için ikiz yapılı bir üçgen mikro-şerit yama anten geliştirdi. M.Deepu Kumar ve diğerleri [7] ikili frekans çalışması elde etmek için bir iki-kaplı mikro-şerit anten geometrisi geliştirdi. Anten geniş bir bant genişliği ile kapılar arasında mükemmel yalıtım sağladı.

K.M. Luk ve diğerleri [8] %26'lık bant genişliğine sahip 8 dBi kazanılı bir ikiz dairesel çanak anten tasarladı. İkiz düzenlemenin dip yamasında dört doğrusal yuva kullandılar. K.M. Luk ve diğerleri [9] ayrıca bir L-biçimli prob beslemeli geniş bantlı dikdörtgen mikroşerit yama anteni de araştırdı. Önerilen antende bir köpük katmanı destek katman olarak kullanıldı. Bu katman dalga boyunun %10'u civarında bir kalınlığa sahipti. Anten %35 oranında bir empedans bant genişliğine ve 7.5 dBi'lik bir ortalama kazanca sahipti.

Y.X. Guo ve diğerleri [10] bir U-yuva dairesel yamalı L-prob besleme ile alt katmanı destekleyen bir köpük katman kullandı. Bu yapıda %38'lik bir empedans bant genişliği ile 6.8dBi kazancı elde edildi. Kin Lu Wong ve diğerleri [11] yüksek çalışma frekanslarında zayıf eş yönlü ışıma karakteristikleri sorununun üstesinden gelmek için geniş bantlı eş yönlü metal plakalı monopol anten geliştirdi. Bu anten basit bir basamak biçimli yapıya sahipti ve uygulaması kolaydı.

W.L. Stutzman ve G.A. Thiele, geniş bant genişliğine ulaşmak için ince bir tel kullanmak yerine düz bir metal kullanmayı önerdi [12]. Son on yılda düz plaka ışıyıcılar için çeşitli geometriler ortaya atıldı. Bununla birlikte bu antenlerin empedans bant genişliklerinin üst uçlarındaki bozulmalar dikkate alınmalıdır. S.Y. Suh ve W.L. Stutzman [13]'de ve S.-Y. Suh [14]'de düzlemsel ters çevrilmiş konik anten denilen yeni bir geniş bantlı, her yönlü, düz anten geliştirdi.

Basit yapıları ve tüm yönlü ışınımları nedeniyle monopoller ve çeşitleri daha fazla dikkat çekmiş ve bant genişliklerini arttırmak için daha fazla çaba gösterilmiştir. Kawakami, H. ve Sato, G[15] Nakano ve diğerleri, [16] Rogers, S.D. ve Butler, C.M.N [17] ile Cho, W ve diğerleri [18] tarafından konik ve çatısal konik, kafes ve çeşitli yüklü monopoller, disk yüklü ve ters F antenler sunulmuştur. Ancak, konik veya dönel simetrik monopollerin hacimli yapısı onların en büyük dezavantajı olarak yorumlanabilir. Son zamanlarda, düzlemsel monopollerin sunulmasıyla tel elemanlar Brown, O.H. ve Woodward, O.M [19] Amman, M.J ve diğerleri, [20], [21] Agrawall ve diğerleri, [22] Chen, Z.N [23] tarafından düzlemsel elemanlarla değiştirildi. Bu yapılarda yatay ışınım düzenleri asimetrik yapıları nedeniyle eş yönlü değildir. Ayrıca, geniş bantlı monopollerde E-düzlemi boyunca ışın demeti gözlenebilir.

Daha küçük boyutlara talep bu alandaki araştırmacıları standart küçük şeritli yamadan daha küçük boyutlu antenler tasarlamak için çaba göstermeye yöneltti. Bu çabalar düzlemsel ters F antenleri ve yamal antenler için yüksek-dielektrik sabitli alt tabaka gibi yeni anten tasarımları getirdi. Aynı zamanda bu antenler geleneksel yamalı antenlerden daha küçüktü ancak herhangi bir bant genişliği iyileştirmesi sunmuyordu. [24]'te J. Michael Johnson ve Yahya Rahmat-Samii tab monopol denilen yeni geliştirmiş bir düzlemsel anteni tanıttı. S. Honda ve diğerleri [25] 1:8 empedans bant genişliği ve tüm yönlü ışınım düzenine sahip bir disk monopol anten sundu. M. Hammoud ve diğerleri [26] geniş bantlı bir disk monopolünün giriş empedansını eşleştirme üzerine bir araştırmayı sundu. N.P. Agrawall ve diğerleri [27] 1998 yılında geniş bantlı düzlemsel monopol antenleri önerdi. P.V. Anob ve diğerleri [28] 2001 yılında uluslararası bir sempozyumda yarı dairesel tabana sahip geniş bantlı dikey bir monopol anteni tanıttı. M.J. Amman [29] bir eğim verme tekniği kullanarak geniş bantlı düzlemsel monopol antenin empedans bant genişliğinin kontrolünü sundu. M.J. Amman ve Z. N. Chen [30] çoklu bantlı kablosuz sistemler için geniş bantlı monopolü geliştirdi. S.-Y. Suh ve diğerleri [31]çoklu-geniş bantlı monopol disk anteni tanıttı. E. Antonino-Daviu ve diğerleri [31] geniş bantlı çift beslemeli düzlemsel monopol anteni önerdi.

A.Khidre ve diğerleri [33], 67mmx74mm büyüklüğünde bir Rogers RT\Duroid alt katman üzerinde geniş bantlı U-yuva yama prob beslemeli bir anten sundu. 2012'de H. Malekpoor ve S. Jam, 50mmx50mm ebatlarında bir ultra-geniş bantlı kısaltılmış yama yapı tanıttı [34]. N.Ghasemi ve diğerleri 2007'de 7.6GHz bant genişliğine sahip bir çok katmanlı prob beslemeli bir yapı tanıttı [35]. Ek olarak Ghannoum ve diğerleri UWB sektörsel uygulamaları için iki E-biçimli ikiz yamalı 55mmx55mm ebatlarında bir mikro-şerit yama anten tanıttı [36]. Bunlara ek olarak son yıllarda yurık kullanmak [37], DGS (Defected Ground Structure) [38], EBG (Electromagnetic Band Gap) yapıları kullanmak gibi pek çok yöntem tanıtıldı ve test edildi.

Bu çalışmada UWB bant genişliğini korurken antenin büyüklüğünü düşürmek için uygun yurıklara sahip bir yedigen (heptagon) yama tasarlanmıştır. Bu anten basit bir biçime sahip ve geçmişte önerilmiş olan antenlerin çoğuna kıyasla imal edilmesi kolaydır. Önerilen antenin ebadı, çoğu UWB uygulaması için yeterince küçük bir FR4 alt katmanı üzerinde 30mmx30mm'dir.

Bu çalışmada simülasyon işlemleri için HFSS (High Frequency Structure Simulator) yazılımı kullanmıştır.

1. INTRODUCTION

Talking about wireless technologies is meaningless without considering antennas. Good and reliable wireless connection requires enough transmitting power, enough bandwidth, and etc. In order to provide these requirements, every part of a system should work well and antenna as the beginning or ending part of a system playes an important role. Since, the first steps of electromagnetic waves recognition, antennas known as a metallic element and different types of them introduced to the world. These last years, by introducing microstrip technologies, microstrip antennas became as a part of interest in industry and academia. Among these revolutions in technology, there was an increasing demand for miniaturizing components, providing more bandwidth to transmit more information, higher data rates and etc. These demands on the other hand caused frequency bands saturation. So, technology needed another revolution to overcome these problems.

Ultra Wideband is one these revolutionary technologies that introdeced to overcome the aforementioned problems. It tries to solve problems by reusing the occupied bands, 3.1 to 10.6 GHz, but at very low power transmition. This technique, Using low transmitting power, makes it invisible for other narrow band radio systems and allows to share the used spectrum. It needs to notice that implementing UWB technologies is very complex, since the devices need to work fast enough with the ability of working in very low power. So, the antennas in these systems need to operate in ultra broadband spectrum with the ability to receive and transmit in a low power.

1.1 Purpose of The Thesis

In this thesis, we will work on developing microstrip antenna for UWB applications. In today's life the size of devices is an important matter. So, it's tried to reduce the size while keeping the bandwidth constant to cover most of the UWB applications. Since, fabrication expenses play a pivotal role in industry, antennas will be designed and fabricated on the substrate of FR4.

In this work it's tried to utilize different methods such as using proper patch shape and implementing slots to reduce the size of proposed antenna with still providing UWB frequency band range.

1.2 Literature Survey

Looking to the some of previous works in recent years; the concept of multilayer substrate antennas in order to achieve greater bandwidth reported by Hall et al. [1]. These antennas which provide bandwidth of 16 times more than a standard patch antenna, constructed on alumina substrates with increased overall height. Another method introduced by C.Wood to locate capacitively excited short circuit parasitic elements at their radiating edges. This method, doubles the bandwidth of microstrip patch antennas [2].

Demeryd and Karlssson [3] by using thicker substrates of low dielectric constant, made a broadband microstrip antenna. This is used as antenna element in an array for broadband operation. Assuming circular patch antennas as a basic broadband antennas, N. Das and ChateIjee [4] itroduceded a conical microstrip antenna with much larger bandwidth. The design of this antenna is based on the modification of the circular patch antenna by slightly depressing the patch configuration conically into the substrate.

Sabban [5] reported a stacked two layer microstrip antenna as a base element of an 64 element Ku band array with 15% bandwidth increasement. Bhatnagar et al. [6] introduced a stacked configuration of triangular microstrip patch antennas to increase the bandwidth. M.Deepu Kumar et al. [7] developed a dual port microstrip antenna geometry to obtain dual frequency operation. The antenna provided wide bandwidth and excellent isolation between ports.

K.M. Luk and *et al*. [8] designed a stacked circular disc antenna using proximity fed technique with bandwidth of 26% and gain of 8 dBi. They used four linear slots in the bottom patch of the stacked arrangement. K.M. Luk and *et al*. [9] also investigated a broadband rectangular microstrip patch antenna with an L-shaped probe fed. In the proposed antenna a layer of foam is used as supporting substrate. This laye had a thickness of around 10% of the wave length. The antenna has an impedance bandwidth of 35% and an average gain of 7.5 dBi.

Y.X Guo and *et al*. [10] used L-probe feeding with a U-slot circular patch and a layer of foam that supported substrate. In this structure, an impedance bandwidth of 38% and gain of 6.8dBi obtained. Kin-Lu Wong and *et al* in [11] in order to overcome to the problem of poor omnidirectional radiation characteristics in high operating frequencies, reported Broadband Omnidirectional Metal-Plate Monopole Antenna. This antenna had a simple step-shaped structure and is easy to implement.

W. L. Stutzman and G. A. Thiele proposed to use a flat metal instead of a thin wire structure in order to achieve wide bandwidth [12]. In last decade, various geometries for flat plate radiators have been presented. However it needs a notice that these antennas suffer from pattern degradation at their high end of impedance bandwidth. S.-Y. Suh and W. L. Stutzman in [13] and S.-Y. Suh in [14] introduced a new wideband, omni-directional, flat antenna called the planar inverted cone antenna (PICA).

Monopoles and their variations due to their simple structure, pure polarisation and omni-directional radiation, atracted more attentions and efforts to increase the bandwidth of them. Conical or skeletal conical, cage, and various loaded monopoles, disc loaded and inverted F antennas have been presented by Kawakami, H., and Sato, G[15] Nakano and *et al*,[16] Rogers, S.D., and Butler, C.M. N [17] and Cho ,W and *et al* [18]. However, the bulky structure of conical or rotationally symmetric monopoles can be interpreted as their major drawback. Recently, by introducing planar monopoles, the wire elements have replaced with planar elements by researchers such as Brown, O.H., and Woodward, O.M [19] Ammann, M.J et al,[20], [21] Agrawall et aI, [22] Chen, Z.N [23]. In these structures horizontal radiation patterns are not omni directional because of their asymmetrical structure. Furthermore, along the E-plane, beam squinting can be observed in broadband monopoles.

Demands for smaller components lead th researchers in this field to devote efforts to design antennas with smaller size than the standard microstrip patch. These efforts brought new antenna designs such as Planar Inverted F Antennas (PIFA) and high-dielectric constant substrate for patch antennas. Also, these antennas were smaller than the traditional patch antennas, but they didn't represent any bandwidth improvement. In [24] J. Michael Johnson and Yahya Rahmat-Samii reported a newly developed planar antenna called the tab monopole. S. Honda and *et al* [25], presented a disc monopole antenna with 1:8 impedance bandwidth and omni-directional radiation

pattern. M. Hammoud and *et al* [26] reported an investigation on matching the input impedance of a broadband disc monopole. N. P. Agrawall *et al* [27] proposed Wide-band planar monopole antennas, in 1998. P. V. Anob *et al* [28] reported a wideband orthogonal square monopole antenna with semi-circular base at an international Symposium in 2001. M. J. Ammann [29] presented control of the impedance bandwidth of wide band planar monopole antennas using a beveling technique. M. J. Ammann and Z. N. Chen [30], has reported wideband monopole antenna for multi-band wireless systems. S.-Y. Suh *et al* [31] has reported multi-broadband monopole disc antenna. E. Antonino-Daviu *et al* [32], proposed Wideband double-fed planar monopole antennas.

A. Khidre and *et al.* [33] presented a wideband U-slot patch probe fed antenna on a substrate of Rogers RT\Duroid with the size of 67mm×74mm. In 2012, H. Malekpoor and S. Jam reported an ultra-wideband shorted patch structure by the size of 50mm×50mm [34]. N. Ghasemi and *et al.* in 2007 presented a multi-layer probe-fed structure with bandwidth of 7.6GHz [35]. Furthermore, Ghannoum and *et al.* presented a microstrip patch antenna with two E-shaped stacked patches for UWB sectoral applications with the dimensions of 55mm×55mm [36]. In addition to these, lots of techniques such as Using slots [37], implementing Defected Ground Structure (DGS) [38], Electromagnetic BandGap (EBG) structures [39] have been introduced and tested in recent years.

In this thesis, a heptagon patch with proper slots is employed to reduce the size of the antenna while keeping the UWB bandwidth. Uniform ground plane, prevents back lobs in radiation pattern and makes it suitable for some applications such as medical usages. All the simulations had been done using HFSS software. This antenna has a simple shape and easy to fabricate in comparison with most of the previously proposed antennas. The size of the proposed antenna is 30mm×30mm on a substrate of FR4 which is small enough for most of UWB applications.

1.3 Hypothesis

Lots of theories and investigations have been developed so far. Among all these, there are some hypothesis which can be base of our work.

First, various shapes of patch is an important factor to obtain the desired bandwidth and radiation. Among all common shapes, circular patch has an intrinsic wideband characteristics. So, by investrigating different shapes the desired UWB, bandwidth can be achieved.

Second, different feeding techniques and methods have been introduced and each one will has its own application. Probe feeding method is known for its narrow bandwidth characteristics. Increasing height of the substrate and proper uses of slot can overcome this limitation.

2. ULTRA WIDEBAND TECHNOLOGY

It is not possible to talk about Ultra-wideband antennas without understanding the meaning of the Ultra-wideband, technologies behind it, its various applications, regulations and also standards that governing it. This chapter presents Ultra wideband (UWB) technologies and explains different approaches used to cover its requirements. The technology itself, without its implementation would be meaningless; therefore, methods of implementation and main applications of this technology will be described briefly. In order to clearly understanding the measurement techniques to fulfill the standards requirements section 2.5 of this chapter deals with this issue.

2.1. Ultra Wideband Systems

Demands for higher data rates, frequency spectrum saturation, low power consumption, and etc. are some of the reasons which put the Ultra wideband in the center of interest during past years. Ultra wideband, in comparison with narrowband systems, uses a large bandwidth for transmitting data. Power usage over the band is much lower than narrowband systems, as illustrated in Fig. 2.1(a). Consequently, because the power of ultra wideband can be interpreted as a noise in narrowband systems using the same spectrum, due to their noise levels, there will be no interference. This fact makes it possible to share the spectrum and space with other established technologies.

The Federal Communications Commission (FCC) first defined UWB as any system having a bandwidth of at least 500 MHz or a fractional bandwidth larger than 0.20. Fractional bandwidth is defined as:

$$band\omega idth = 2\frac{f_H - f_L}{f_H + f_L} \qquad (2.1)$$

where f_H is the higher and f_L is the lower frequencies of operation. These frequencies are defined as the points where the power is reduced by -10 dB from the frequency with maximum power f_M.

In 2002, the FCC allowed unlicensed UWB transmission in the frequency band between 3.1 to 10.6 GHz.According to the defined standards, inside the frequency band, the Effective Isotropic Radiated Power (EIRP) should be below -41.3 dBm.
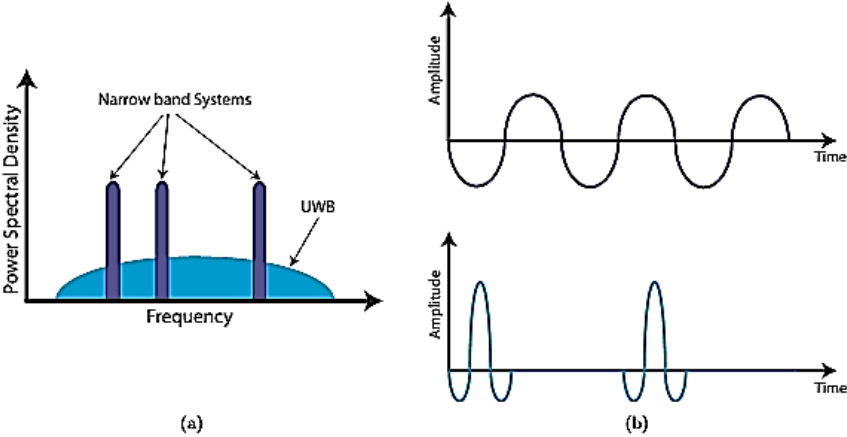

Figure 2.1 : Gain pattern of narrow band and Ultrawide band systems: (a) Frequency domain, (b) Time domain.

In recent years, industry and academia focused on two different approaches in order to cover the ultra wideband. Using several subbands to cover the whole band is the first approach. The second, consists in sending very narrow pulses having the desired bandwidth. Following subsections describe these two methods.

2.1.1. MB-OFDM

MultiBand Orthogonal Frequency Division Multiplexing (MB-OFDM) based on dividing the frequency spectrum in several sub bands using different carriers. Industry paid lots of attention to this approach and it is more widely used technique. Just after the FCC assigned UWB frequency allocations, WiMedia Alliance [40] was founded in September 2002. It has today more than 350 members, among who are some of the most renowned companies, and is maybe the strongest promoter of UWB standardization around the world.

2.1.2. IR-UWB

The second method suggests that in order to cover broad spectrum in Figure 2.2(a), very short pulses in time can be used, see Figure 2.2(b). This type of UWB is called Impulse Radio UWB (IR-UWB) [41], and consists in sending pulses or a group of pulses representing one bit of a coded signal. Covering the spesification of FCC would

mean that the pulses should be at least 2 ns wide (BW = 500 MHz) and have small amplitude due to low transmitted power rule.

Time dependency and complexity of implementation put this approach far from industry interest, but the favorite of researchers in universities or investigation centers.

2.1.2.1. Modulation

In order to send the information of impulse signal, several modulation techniques introduced. Figure 2.2 shows the most studied with higher possibilities of implementation methods. A small description of each technique is given below.
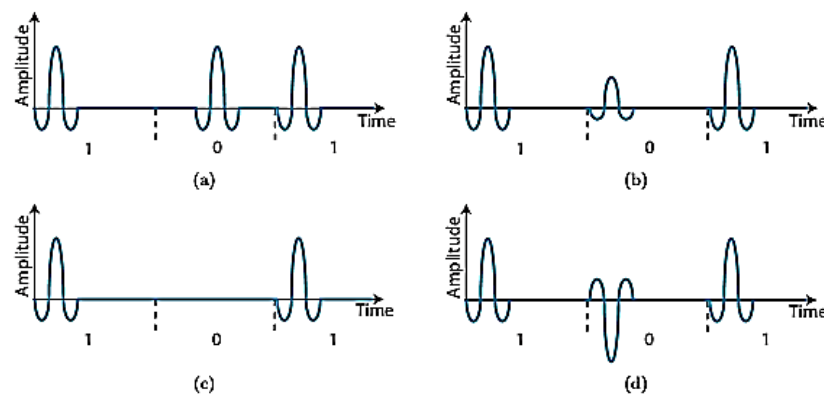

Figure 2.2 : Modulation techniques of IR-UWB: (a) PPM, (b) PAM, (c) OOK, and (d) BPSK.

- **PPM** − Pulse Position Modulation can be interpreted as the most common modulation scheme used for IR-UWB. In this technique, pulses are sending at different times, and each position represents a different bit value. In Figure 2.2 (a), at the beginning a 1 is sent whereas the 0 is sent in the middle of the period.
- **PAM** − Pulse Amplitude Modulation uses pulses with different amplitudes; each amplitude is related to a specific bit value. In Fig. 2.2 (b), a 1 has higher amplitude than the bit representing the 0.
- **OOK** − On-Off Keying is the simplest modulation and the less power consuming. A pulse means a 1 while the absence of a pulse is 0, as shown in Fig. 2-2 (c).
- **BPSK** − Binary Phase Shift Keying consists of changing the phase of the pulse, according to the bit value to be transmitted. A 1 has 180∘ phase difference from a 0. Fig. 2.2 (d) shows a 1 having positive amplitude and a 0 that has the same magnitude but negative.

9

Depending on the type of information or the transceiver to be used, more complex modulations are avaiable.

2.1.2.2. Pulse shapes

One of the most experienced areas in UWB pulses is Radar technology [42], [43], generating high power pulses in the order of kV. From the antenna point of view, low power ultra wideband waveforms are an important topic of study [44] as well as from the generator approach [45]. The priors were investigating an optimum pulse to transmit without distortion. Now, researchers are looking for low power technologies that can generate such pulses.

There are various types of pulses that can cover the UWB [46] within the FCC Spectrum mask. The most common pulse shapes, are described below.

o **Gaussian Signals** − The Gaussian pulse is described using the exponential:

$$T(t) = Ae^{-\frac{t^2}{\tau^2}} \qquad (2.2)$$

where A is the amplitude, τ stands for the width of pulse and t is the duration of the pulse. Increasing value of τ, means a pulse with larger width. Since, the signal produced using equation (2.2) is a baseband pulse, therefore its central frequency is located at 0 Hz. So, derivative of the pulse needs to be obtained, in order to move the signal to higher frequencies. By increasing the derivative number "n" in the following equation, the signal will achieve higher frequency:

$$T_n(t) = A\frac{d^n}{dt^n}e^{-\frac{t^2}{\tau^2}} \qquad (2.3)$$

▪ **Carrier-Based** − Modulating a baseband pulse is a simple way to generate an UWB pulse [47]. This process can be described as up converting the pulse to the targeted frequency. Baseband pulse is generated using pulse generator. Generated pulse multiplied with a signal coming from a local oscillator at a frequency equal to the center frequency of the desired pulse. Figure 2.3 represents this proceeding and its frequency effect on the signal.

According to the application and generating simplicity, the shape of the baseband pulse varies. The length of the pulse is inversely proportional to the bandwidth of the signal. Triangular and square signals can be simply generated

and some integrated circuits have already been implemented which generate this carrier based approach pulse to cover a 500 MHz bandwidth [48].

A carrier based pulse with 528 MHz bandwidth and correct carrier modulation can represent a band on the MB-OFDM allocation. Meaning that a band group of MB-OFDM can be decomposed using two or three carrier based pulses.
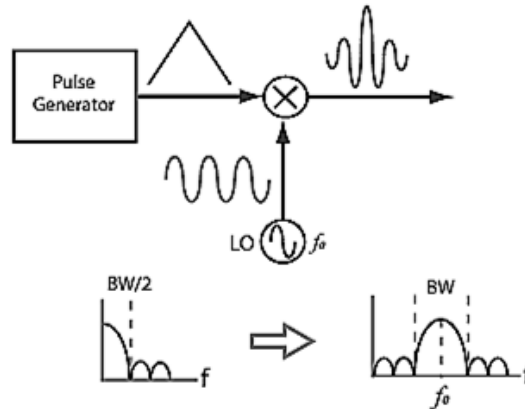

Figure 2.3 : Carrier-based pulse generation.

2.2. Ultra-wideband Applications

Wide range of applications can benefit from the UWB characteristics. according to [49], UWB applications can be grouped in four main classes:

• High-data-rate communications

• Low-data-rate communications

• Imaging

• Automotive radar

As soon as the UWB technologies approved by the FCC, many applications have been investigated. Its unique characteristics such as: low power, narrow pulses, and etc. gained a lot of attention and many reasearches focused on the benefits that this technology can provide. Among all the applications that are studied today, the most innovative and demanded by antenna designers are presented below:

- **WUSB** − Based on the Wi-Media Alliance's UWB common radio platform [40], Wireless Universal Serial Bus (WUSB) developed which is capable of transmitting at the rate of 480 Mbit/s at distances up to 3 meters and 110 Mbit/s at up to 10 meters. Intel introduced the second generation of these devices (USB

2.0) that is already available in the market [50]. This application is one of the favorite studies in the antenna domain because of its small size and large capabilities [51], [52]. Monopole and dipole antennas are appropriate for this application because it is requiring small antennas with omnidirectional radiation pattern.

▪ **UWB Radar Imaging** − is a hot field of study, especially in detection systems of unwanted objects. Being capable of detecting landmines put Ground Penetrating Radar (GPR) in the center of interest [53], [54]. Expanding applications of UWB imaging systems into the biomedical domain in comparison with aggressive X-Rays can be very useful in cancer detection due to its good penetration and resolution characteristics [55]-[58]. Array antennas with directional elements mainly used for their higher gain. However, Microstrip patch array antennas due to their small sizes put themselves in the center of interest [59].

▪ **Ranging** – Small pulses means good time resolution of UWB signals. This feature can provide various applications high resolution ranging [60]. Among many features of wireless networks, ranging and location awareness can name as much desired features that in some applications such as tracking, finding people, safety, emergency, and robotics [61]. Since, there might be multiple reflections pulse distortion is defined as an important factor that should be avoided. This issue demands a good antenna design as a foundation of work [62].

Wireless Local Area Networks (WLAN), Personal Area Networks (PAN), high precision location RFID, home entertainment and multimedia interfaces can be also as a part of UWB communication.

2.3. Power Measurements

In addition to the ultra bandwidth as main feature of UWB technologies, low transmission power is also one of the fundamental specification of this new technology. In order to avoid interference between various UWB systems, power restrictions vary. These restriction are chosen accordding to the region characteristics and power restrictions varies from a place to the other but there is no doubt that it is much lower than narroband technologies.

For measuring the emission power, the ITU-R recommends a distance of 3 meters. It is obvious that the recommeded distance can be modified in a case that the signal is too weak. However, it's not allowed to cross into the farfield region of antenna. So, the measurement distance should satisfy the following equation that shows the farfield region restriction:

$$R > \frac{2D^2}{\lambda} \tag{2.4}$$

where R is the distance in meters, D is the aperture of the antenna or diameter of the sphere enclosing the device under test, and λ is the wavelength.

Frequency domain measurements are usually done using a spectrum analyzer. Figure 2.4 illustrates its main components. The spectrum analyzer displays all harmonics of the input signal. This process is done by sweeping an IF filter over all the frequencies containing the pulse. Its resolution bandwidth (RBW) should be wisely defined, in order to measure the correct power spectrum of the signal.
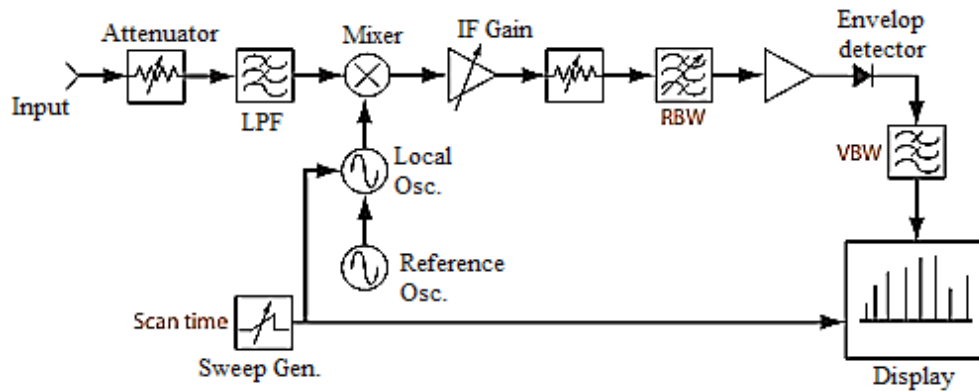

Figure 2.4 : Schematics of a vectror Network Analyzer.

Figure 2.5 can define the peak and average powers. The average power is defiened as the muliplication of peak power and the duty cycle:

$$P_{avg} = P_{peak}\frac{\tau_{eff}}{T} = P_{peak}\tau_{eff}PRF \tag{2.5}$$

Written as a ratio in dB:

$$\frac{P_{avg}}{P_{peak}} = 10\log_{10}(\tau_{eff}PRF) \tag{2.6}$$

Considering the RF pulse in Figure 2.5, 1/T is its pulse repetition frequency (PRF). The IF filter's bandwidth can be manually set in the spectrum analyzer. When RBW is smaller than PRF (Figure 2.6 (a)), the display shows frequency domain of the actual Fourier components of the input signal. When the RBW is larger than the PRF (Figure 2.6 (b)), the display shows the Fourier transform response of the pulsed signal. In [63], the first setup is known as a "Line" spectrum and the second is named "Pulse" spectrum.
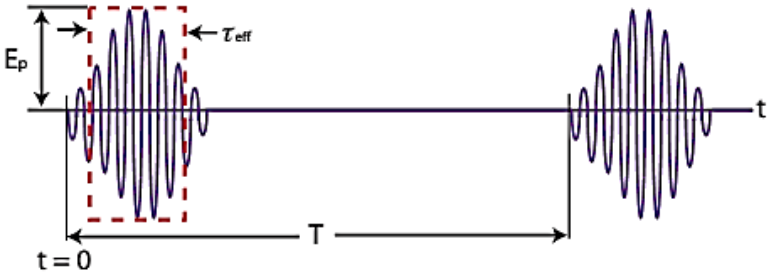

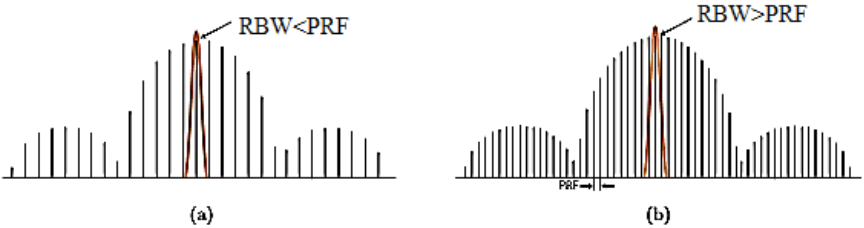**Figure 2.5 :** Basic RF Pulse (figure adapted from [63]).

Figure 2.6 : IF bandwidth (RBW) and pulse repetition frequency (PRF): (a) Line spectrum, (b) Pulse spectrum.

The standards define different values of PRF, the smallest value defined by the IEEE as 3.9 MHz. Standard spectrum analyzers have a highest RBW of 3 MHz. Therefore, when measuring an UWB signal, the PRF will be always higher than the RBW. For this reason, the measurements should be done using a "Line" Spectrum setup.

In this setup, the display has the normal true frequency domain characteristics. The amplitude of each line will not change when the RBW is changed as long as it remains considerably below the PRF (RBW < 0.3 PRF). When the width of the pulse τ_{eff} is very small, the power of the modulated signal is distributed over a number of spectral components (carrier and sidebands) and its power seems to be reduced. Each spectral line containing only a fraction of the total power. The reduction in power is given by

the line spectrum pulse desensitization factor α_L, which is equal to the duty cycle τ_{eff} /T in decibels:

$$\alpha_L = 20 \log_{10} \left(\frac{\tau_{eff}}{T} \right) \qquad (2.7)$$

The different setups of the spectrum analyzer required doing the correct peak and average power measurements (using the "Pulse" spectrum setup) will be given in the following subsections. The exact definitions of the EIRP, peak power and average power, given by the FCC and IEEE are given, as well as the proposed limitations.

2.3.1. EIRP

Acording to the "IEEE Standard Definitions of Terms for Antennas", EIRP is defined as [65]:

"In a given direction, the gain of a transmitting antenna multiplied by the net power accepted by the antenna from the connected transmitter."

The FCC in the Title 47 Part 15, subpart F (15.503), describes the EIRP for UWB systems as [63]:

"Equivalent isotropically radiated power, i.e., the product of the power supplied to the antenna and the antenna gain in a given direction relative to an isotropic antenna. The EIRP, in terms of dBm, can be converted to a field strength, in dBμV/m at 3 meters, by adding 95.2. As used in this subpart, EIRP refers to the highest signal strength measured in any direction and at any frequency from the UWB device, as tested in accordance with the procedures specified in 15.31(a) and 15.523 of this chapter."

The EIRP value can be calculated by

$$EIRP = P_{in} + G_A \qquad [dBm] \qquad (2.8)$$

where EIRP is given in dBm , P_{in} is the power in dBm measured at the antenna terminal, and G_A is the antenna gain in dBi at a given direction. Then, the field strength at 3 meters is obtained as

$$E|_{3m} = P_{in} + G_A + 95.2 \qquad [dB\mu V/m] \qquad (2.9)$$

2.3.2. Peak power

The FCC defines the limitations of the peak level for while the emissions contained a 50 MHz bandwidth around the frequency of highest emission, f_M. That limit is 0 dBm EIRP. Since the widest bandwidth is 50 MHz, this value was chosen.

However, according to the limitations of spectrum analyzers, it may not be possible to measure the peak power based on a 50 MHz resolution bandwidth. standard spectrum analyzers will provide only 3 MHz as the widest available RBW that can be employed.

2.3.3. Average power

According to the FCC, the average power limitation for an UWB field, with distance of measuring at 3 meters and a 1 MHz resolution bandwidth (RBW), is 500 µV/m. Employing (2.9), can be proved that this value agrees with the average power limitation of the FCC spectrum mask: −41.3 dBm/MHz.

The average power can be calculated using (2.6). This effort adds the peak power and the duty cycle in dB to the formula.

$$P_{avg}[dB] = P_{peak}[dB] + 10\log_{10}\left(\tau_{eff} \times PRF\right) \qquad \textbf{(2.10)}$$

3. UWB ANTENNA CHARACTERISTICS AND FEEDING TECHNIQUES

After considering general concepts of ultra wideband technologies, it is possible to proceed to the main focus of this thesis: Ultra wideband antennas. A short introduction about the antennas' history will be good start for this chapter. The key to understand an antenna and its functioning is electromagnetic radiation. Despite prevalent believes, there is no need to be specialist in integro-differential equations to understand electromagnetic radiation. In order to grasp the concepts of electromagnetic radiation, one only needs to understand the electricity and magnetism. Researches in these fields, goes back to nearly two thousand years. Great scientists worked in these fields to deliver the great results to James Clerk Maxwell, who is the most known person in electromagnetic fields for what are currently called the Maxwell equations.

Maxwell didn't derive all the equations known with his name but he saw the connection between Ampere's, Faraday's and Gauss's law. He showed that by extending Ampere's law using socalled displacement current term, electricity and magnetism became united into electromagnetism. By adding this displacement current term, the equations governing electricity and magnetism allow electromagnetic waves to exist. According to these, Maxwell predicted the existence of electromagnetic waves years before he was proven by the reception of radio waves. These equations that are represented in eq. (3.1) to eq. (3.4).

$$\nabla \times \bar{\varepsilon} = -\frac{\partial \bar{B}}{\partial t} - \bar{M} \qquad (3.1)$$

$$\nabla \times \bar{H} = \frac{\partial \bar{D}}{\partial t} + \bar{J} \qquad (3.2)$$

$$\nabla . \bar{D} = \rho \qquad (3.3)$$

$$\nabla . \bar{B} = 0 \qquad (3.4)$$

$$
\begin{aligned}
where: \quad &\bar{\varepsilon} = Electric\ field\ intensity\ in\ V/m \\
&\bar{H} = Magnetic\ field\ intensity\ in\ A/m \\
&\bar{D} = Electric\ flux\ density\ in\ Coul/m^2 \\
&\bar{B} = Magnetic\ flux\ density\ in\ Wb/m^2 \\
&\bar{M} = Magnetic\ current\ density\ in\ A/m^2 \\
&\bar{J} = Electric\ current\ density\ in\ A/m^2 \\
&\rho = Electric\ charge\ density\ in\ Coul/m^3
\end{aligned}
$$

These equations reveal that the source of electromagnetic radiation is accelerated charge. In real life, we will find accelerating and decelerating charges in time-varying currents. Charge acceleration or deceleration in an electrically conducting, wire object may be found where the wire is curved, bent, discontinuous or terminated. All these origins of radiation are shown in Figure 3.1 [66].
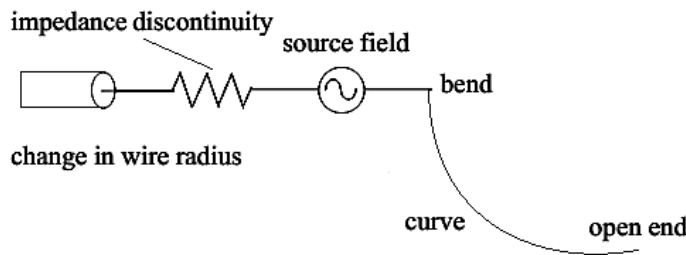

Figure 3.1 : Several origins of radiation on a wire object.

Wire antennas, as well as non-wire antennas, are designed to support oscillating currents. An oscillating current consists of charges accelerated back and forth. These oscillating currents thus create a regular disturbance or continuous radiation.

Heinrich R. Hertz demonstrated the generation of electromagnetic waves in 1886. To experimentally verify Maxwell's theory, Hertz transformed the closed resonance system into an open resonance system. He replaced the bottom coil with a pair of straight wires, at the center connected to a spark gap. The spark gap was connected to the secondary windings of a conduction coil, see Figure 3.2, and the straight wires were equipped with electrically conducting spheres that could move over the wire segments. By charging the two straight wire segments, eventually the breakdown voltage of air is reached and a spark is created over the small air-filled spark gap. This spark makes a pulsed current flow through the two wire segments. Since a pulse signal actually consists of an infinite number of signals of different frequencies (or periods,

T=1/f), the resonant circuit picks out the current with the 'right' frequency and this current will oscillate in the circuit and create the radiation.
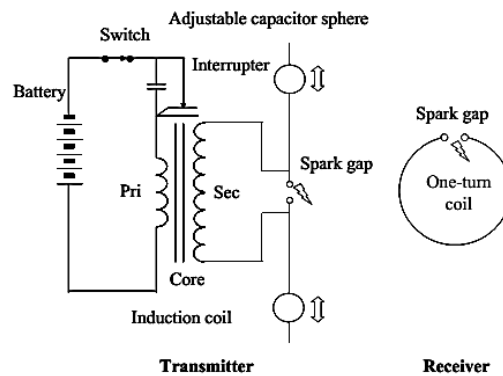

Figure 3.2 : Hertz's open resonator system.

With the receiver (this one-turn loop) placed several meters away from the transmitter (the pair of straight wires with the spark gap), small sparks could be observed in the gap of the receiver when the radiator discharged. His equipment may be regarded as the first radio (transmitter and receiver) system. His transmitter was equipped with the first dipole antenna, his receiver consisted of the first loop antenna working at a distance about 20 meters [67]. In 1901 Marconi introduced the first trans-Atlantic transmission. Marconi was able to transmit short or long pulses a indicators of Morse codes. A large wire antenna connected to ground was used for the purpose. Although the main goal of these wireless pioneers was to transmit narrowband signals, they began radiating Ultra wideband damped impulse signals [68].

This success, was a proof of great use of wireless technologies and a start point for scientists' non-stopable research in order to improve the performance of the radios.

In the 1980's the boom of the mobile telephone revolutionized radio engineers. Technology started to advance at higher pace. New concepts, like frequency reuse concept, presented with the purpose of reducing the number of required channels by optimizing the spectrum usage.

World War II was one of the main science contests that itroduced lots of things for the first time such as tranmitting controlled and desired narrow pulses. RAdio Detection And Ranging (Radar) used by the U.S. Navy. Table 3.1 provides IEEE radar bandwidth allocation. The relation between Radar and UWB is indisputable. Though, radars radiate much power than UWB technologies but using very short pulsed comes

from this technology. Charactrization of radars and the methods of this job are leader of characterizing UWB antennas. Next section of this thesis discusses some parameters used in characterizing Ultra-wideband antennas and the methods used to characterize UWB systems. Some of these methods used in radar applications for the first time.

Table 3.1: Radar IEEE Band Designations

Band Name	Frequency Range
HF	$3 - 30$ MHz
VHF	$30 - 300$ MHz
UHF	$300 - 1000$ MHz
L-band	$1 - 2$ GHz
S-band	$2 - 4$ GHz
C-band	$4 - 8$ GHz
X-band	$8 - 12$ GHz
K_u-band	$12 - 18$ GHz
K-band	$18 - 27$ GHz
K_a-band	$27 - 40$ GHz
Millimeter wave band	$40 - 300$ GHz

3.1. Characterization of Ultra-wideband Antennas

Analysis envoirnment maybe the main difference in studying narrowband or Ultra Wideband antennas. Since the first transmission of RF signals, continues waves which followed by frequency domain technique had been investigated by the engineers and scientists. This technique, frequency domain, is used in narrowband antenna analysis. The following describes a summary of parameters are the most well known and widely used in characterizing antennas.

3.1.1. Antenna matching

One of the main parameters in designing an antenna is antenna matching or antenna impedance matching. This parameter defines the amount of energy that the latter can radiate. According to this parameter, an ideal antenna will be defined as the antenna that radiates all the power injected into its input terminal. As it is discussed in every basic circuitry theories, impedance matching is the fundamental condition to fully transmit the power from one network to the other. Therefore, in antennas just like the other networks, in order to transmit all the power injecting through the port and avoid reflections, the impedance of the antenna should be matched to the input port. Figure

3.3 illustrates this claim. The voltage reflection coefficient of an antenna at the input port can be calculated as:

$$\Gamma = \frac{Z_A - Z_C}{Z_A + Z_C} \qquad \textbf{(3.5)}$$

where Z_A and Z_C are the impedances of the antenna and input port, respectively.

It can be expressed in power as:

$$\Gamma_{dB} = 20\log(\rho) \qquad \textbf{(3.6)}$$

where $\rho = |\Gamma|$. A more commonly used expression instead of voltage reflection coefficient is the return loss, which is defined as the inverse of the power reflection coefficient [69]:

$$Return\ loss = -20\log_{10}\rho \qquad \textbf{(3.7)}$$

Another parameter while discussing about the antenna impedance mismatch is the Voltage Standing Wave Ratio (VSWR)

$$VSWR = \frac{1+\rho}{1-\rho} \qquad \textbf{(3.8)}$$

Typical return loss value is 10 dB as a limit in the lower and higher edges of the band. Bandwidth of an antenna can be identified from its return loss. A narrowband antenna represents its best impedance matching at the resonant frequency while a broadband antenna, might have multiple resonances and a good matching in its operating bandwidth.
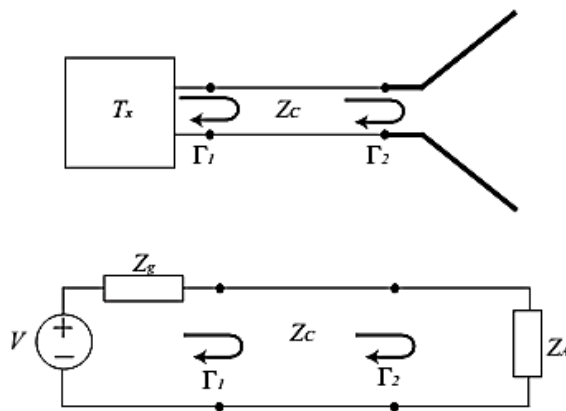

Figure 3.3 : Antenna reflection coefficient in transmission and circuit representation (Figure adapted from [69]).

voltage reflection coefficient, return loss and VSWR can easily be measured using a network analyzer. Although simulations of this parameter are very accurate but there might be differences between simulation and measurements of the antenna due to its structure and size. Small antenna will show lots of discrepancies in measurement so, there is a need for special attention during tests.

3.1.2. Radiation pattern

Graphical presentation of antenna's radiation as a function of space coordinates named radiation pattern[67]. Analizing an antenna in frequency domain leads to characterize radiation pattern by its directivity or gain. Definition of the directivity of an antenna is:

$$D = \frac{U}{U_0} = \frac{4\pi U}{P_{rad}}$$ (3.9)

Where U and U_0 stand for radiation intensity at a given direction from the antenna and the radiation intensity averaged over all directions in a sphere, respectively. P_{rad} is the total power radiated by the antenna [70].

The other useful parameter for an antenna is its gain that brings the antenna radiation efficiency *e* in consideration. According to the definition presented in [70], losses arising from impedance and polarization mismatches may not take into account in gain. It is then related to the directivity with:

$$G=eD$$ (3.10)

Radiation patterns are normalized with respect to an isotropic antenna, thus the values of directivity and gain are represented in dBi. Figure 3.4 presents ideal radiation patterns of a directional and an omnidirectional antenna. The radiation patterns are calculated in different frequencies that is indicated by different lines in figure 3.4.

For measring radiation pattern, there is a need for anechoic chamber that all test are done inside it, in given number of frequencies. Again, small antennas would cause measurement inaccuracy and need special attention.
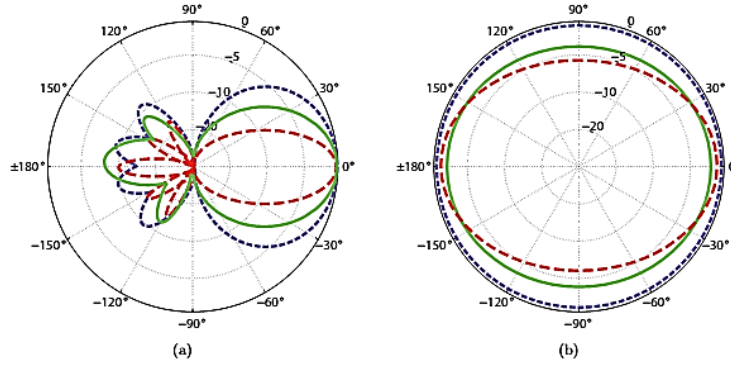
Figure 3.4 : Radiation pattern of an: (a) Directive antenna, (b) Omnidirectional Antenna.

3.1.3. Radiation efficiency

The ratio of the total power radiated by an antenna to the net power delivered to the antenna is called radiation efficiency [70].

$$e = \frac{P_{rad}}{P_{in}} = \frac{P_{rad}}{P_{rad} - P_{loss}} \tag{3.11}$$

where P_{loss} is the power loss in the antenna structure, P_{rad} the radiated power and P_{in} the input power at the antenna terminals.

Wheeler cap method are widely used to calculate the efficiency of narrowband patch antennas [71], [72]. The cap is a metallic or conducting hemisphere surrounding the antenna. The antenna is located inside the cap with a ground plane common to both structures. In 2005, H. Choo and *et al*, measured the impedance of an antenna with and without the cap and so the efficiency caculated as [73]:

$$e = \frac{R_{nocap} + R_{cap}}{R_{nocap}} \tag{3.12}$$

The presented method works only for resonant antennas that have a characteristic impedance of the type RLC. It's worth of notice that resonant frequency determines the size of the Wheeler cap, which can calculated as: $r \approx \lambda/2\pi$ [74]. Chooa and *et al*, in their paper in addition to the peresented calculation, investigated the effects of the size and shape of cap by replacing hemisepheres cap with a cubic caps [73]. In the following sections calculation methods for efficiency of UWB antennas will be discussed.

Nowadays, radiation efficiency can be calculated using different simulation tools.

Various parameters are used to describe different characters of UWB antennas. Some of these methods are as just mentioned which are using for narrowband antennas. But, there are some methods that have been developed and framed only for wideband antennas characterization which may or may not transmit short pulses (IR-UWB or MB-OFDM). Radiating short pulses with duration of nanoseconds, and having a bandwidth of more than 100% in radars, made them as a great opportunity to perform various methods [75]. With the advent of UWB technologies in 2002 and defining its properties such as using short pulses, these characterization methods were applied to this newborn tech and new methods started to be investigated.

Following sections present a summary of the most commonly used characterization procedures of UWB antennas. It is also need to be stated that time domain techniques introduced by introducing UWB systems and so, the methods will employ both frequency or time domain simulationing tools or measurements.

Investigation in [76] and [77] had been focused on Wheeler cap method with the purpose of introducing new methods to calculate the efficiency over a wider bandwidth. In this method, a larger cap than the one needed for narrowband antennas is used. "UWB Wheeler Cap" method that is introduced by Schantz in [77], designed based on free radiation of antenna in the cap so, it will receive its own reflected signal.

Power fractions, are separated parts of the power budget that will describe as:

a) Fraction of the input power is dissipated in losses ($l = P_{loss}/P_{in}$),
b) Reflected fraction due to mismatch ($m = P_{reflected}/P_{in}$)
c) Radiation fraction ($\eta = P_{rad}/P_{in}$).

It's clear that sum of these fractions over a suitable time interval and applying conservation of energy gives: $l + m + \eta = 1$. Figure 3.5 shows the power budget of two antenna systems. According to this, receiving antenna (Rx) can obtain all the radiated power. The factor ηm represents reflected power of transmitting antenna at the Rx antenna terminals.
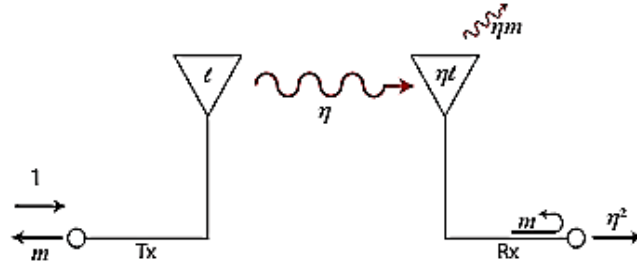
Fig. 3.5 Power budget for a Tx-Rx antenna pair. (Figure adapted from [77])

By locating receiver antenna inside the Wheeler cap, reflected signals from the cap are only singlas that the antenna receives (Figure 3.6). These reflections of the cap, are almost ideal time reversal of the transmitted signal. Therefore, we can replace the reflection coefficent of free space with the reflected power inside the UWB wheeler cap (m = $|S_{11FS}|^2$). So, the scattering parameters inside the UWB Wheeler cap can be calculated as:

$$|S_{11WC}|^2 = m + \eta^2 + \eta^2 m^1 + \eta^2 m^2 + \eta^2 m^3 \ldots = |S_{11FS}|^2 + \eta^2 \sum_{n=0}^{\infty} |S_{11FS}|^{2n} =$$

$$|S_{11FS}|^2 + \eta^2 \frac{1}{1 - |S_{11FS}|^2} \qquad (3.13)$$

where S_{11FS} and S_{11WC} indicate the reflection coefficients of free space and inside the UWB Wheeler cap, respectively.

Therefore, the radiation coefficient η becames:

$$\eta = \sqrt{(1 - |S_{11FS}|^2)(|S_{11WC}|^2 - |S_{11FS}|^2)} \qquad (3.14)$$

All these calculation based on this assumption that inside the Wheeler cap, the reflections are orthogonal to each others.

Radiation efficiency in most of the simulation tools can be calculated just in a given frequency. However, by implementing the Wheeler cap inside the simulation environment, the efficiency can be calculated from the antenna return loss inside the cap and in free space [78]. There are also some other methods based on time domain measurements inside a reverberation chamber [79], [80] that enables us to take multiple reflections into the account inside the chamber.
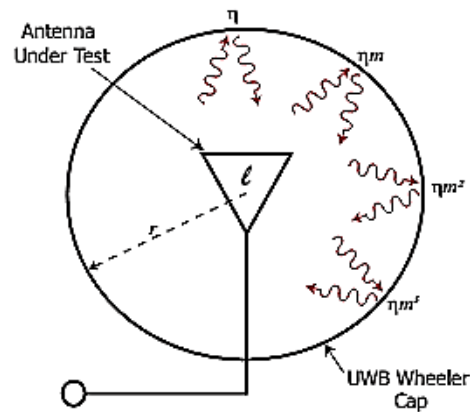
Figure 3.6 : Reflections inside UWB Wheeler Cap. (Figure adapted from [77])

3.1.4. Gain pattern

One of best ways to discuss about directivity or gain is to plot them in a polar plot. This action usually is done in a given frequency for different radiation planes ,seprativly. This representation will show the form of radiation around the antenna, Hence it is called "Radiation Pattern" (as discussed in section 3.1.2). It is clear that we can easily talk about the type of antenna and its radiation form just by seeing the radiation pattern. As discussed above, if radiation pattern looks like Figure 3.4(a) the antenna will called directive. These antennas have a main lob that radiates more at a given angle than the other angles. If the antenna is an omnidirectional antenna, its pattern will be look like Figure 3.4(b) and it will radiate almost equally in all directions. As mentioned above, the radiation pattern can be calculated and plotted at a selected frequency. Consequently, it will works more well in narrowband antennas because, their radiation pattern would not be affected by frequency changes. However, this tool, plot of radiation pattern, is used to characterize UWB antennas as well. It's clear that, it is not possible to plot it for every single frequency but it is logical to plot it at some selected frequencies and expand it to the other middle frequencies.

Gain pattern, is one of the main representation of changes in gain over the frequency and angle. This plot is countor plot which its base consists a 2D plot of frequency versus angle and the antenna gain added as the third parameter to it. This representation of gain will provide desired information in any frequency or angle and makes it possible to easily identify the best or worst radiation frequencies and angles. According to this, an ideal omnidirectional antenna should present a plot with a

constant color in whole the diagram. This clearly means that the gain is independent from the frequency and angle. So, there is no doubt that a directional antenna should provide a diagram in a multi color way which is showing higher gain in a concentrated part as a main beam and the other parts should be zero at other angles.

To illustrate the discribed diagrams, simulated gain pattern of a circular monopole as an example for omnidirectional antennas and a Vivaldi antenna as a part of directive antennas are shown in figure 3.7. It can be easily seen that different radiation point, bad or good, are representing in any angle and frequency. As it's expected and also shown in Figure 3.7 (a) the Vivaldi antenna along its main beam direction shows a constant gain over the whole band while it is very low outside the main beam. On the other hand, an omnidirectional pattern for the circular monopole antenna shows almost constant coloring over the whole diagram. Figure 3.7 (b) illustrates this claim clearly. However, there are some very low gain points around 8.2 GHz.
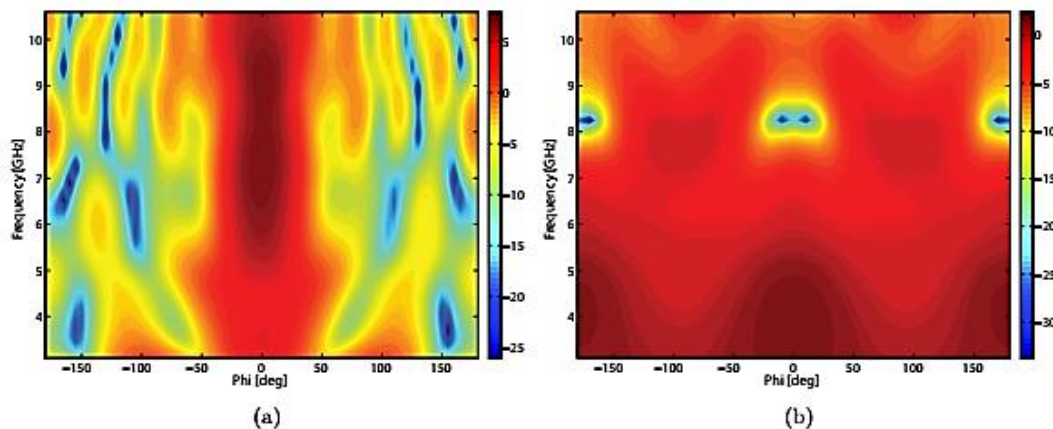

Figure 3.7 : Gain pattern of (a) Vivaldi antenna, (b) Circular Monopole.

3.1.5. Polarization

Orientation of the electric field vector in electromagnetic waves is known as polarization of these waves. By assuming a stationary plane perpendicular to propagating direction and drawing the scheme of electric field changes on it, the figure will represent the polarization. Figure 3.8 illustrates different polarizations in electromagnetic waves. As it's shown, three main classifications for polarization are known: Linear, Circular, and Elliptical.
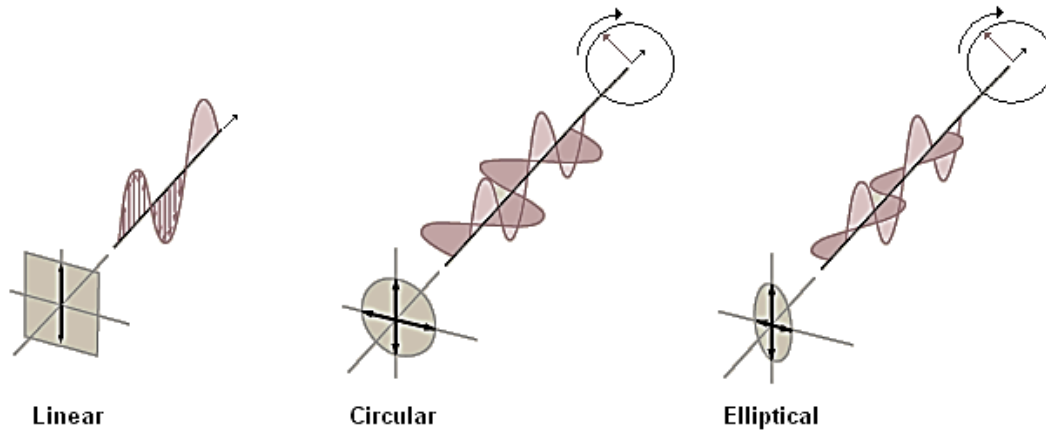
Figure 3.8 : Different polarizations of electromagnetic waves.

Decomposing an electromangetic wave into two prependicular component, also known as Co and Cross components, will be helpful. If both components are equal in magnitude with 90° of phase difference, circular polarization can be achieved. In case of non-equal magnitudes with the phase differnce of 90°, the polarization will be elliptical and if the phase differnce changes, it may lead to linear polarization.

3.1.6. Group delay

Group delay is a parameter that defined for two port devices like filters, amplifiers, mixers, and etc. This parameter is used to measure the absolute delay of the signal and the phase distortion between the input and the output of the device.

Recalling the use of impulse response h(t) in time dmain in circuit theory and moving to the frequency domain lead us to define the frequency dependent complex transfer function H(ω). This function for a given device can be defined as:

$$H(\omega) = A(\omega)e^{j\phi(\omega)} \tag{3.15}$$

where A(ω) is the amplitude and Φ(ω) the phase response of the device.

Now, the group delay would be defined as the derivative of the phase response versus frequency [81].

$$\tau = -\frac{d\phi(\omega)}{d\omega} = -\frac{1}{360°}\frac{d\phi(f)}{df} \tag{3.16}$$

In this equation, a constant value takes the seat of phase response linear portion, and the deviations from linear phase are converted into deviations from constant group

delay. The average of signal through the time that traveles over the device or two ports of system is called average delay [82].

Deviations from linear phase or phase non-linearities will cause signal distortion in communications systems. Usually, in order to characterizing a phase ripple, its maximum peak-to-peak will be measured. However, this measurement never can characterize it completely, because the slope of the phase ripples can be questioned and it can be obtained by counting the number of ripples per frequency unit. Group delay is known as a parameter that takes the mentioned point into account. So, group delay is a good indicator for phase distortion. Figure 3.9 provides an example to illustrate the discussed matter. As it is shown, there are two phases with the same maximum peak-to-peak but with different changes and this means different group delays. In Figure 3.9(a), the small peak-to-peak group delay, means few ripples per frequency unit. On the other hand, in Figure 3.9(b), there are more ripples per frequency unit and hence, a large peak-to-peak group delay will be in hand. The group delay in Figure 3.9(a) is more constant than the one in Figure 3.9(b), having the same phase peak-to-peak.
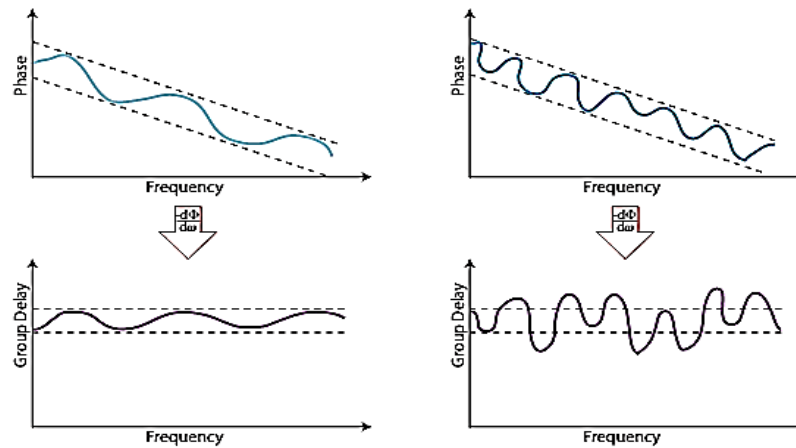

Figure 3.9 : Group delay and its relation to peak-to-peak phase ripple. (Figure adapted from [82])
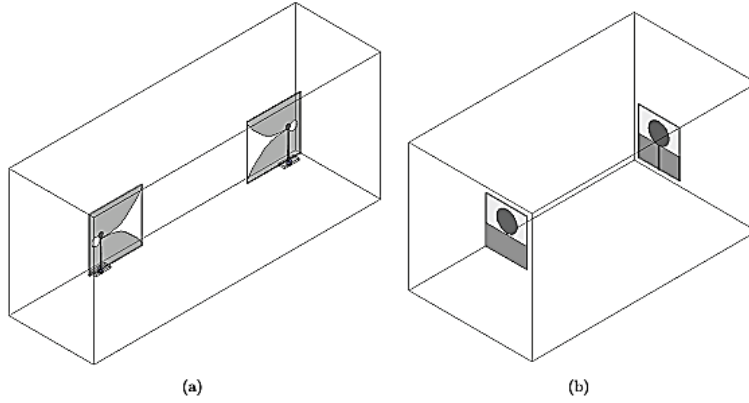
Figure 3.10 : Group delay simulation setup in HFSS.

Group delay can be measured using a Vector network analyzers (VNA). A VNA provides group delay directly by measuring phase [82], [83]. VNAs instead of measuring the differential on (3.16), measure a different quotient. This provides a good approximation if the non-linearity of phase Φ is limited in the observation frequency range, Δf.

$$\tau_g = -\frac{d\phi(\omega)}{d\omega} = -\frac{1}{360°}\frac{\phi(f+\Delta f/2)-\phi(f-\Delta f/2)}{\Delta f} \qquad (3.17)$$

In order to obtain group delay, transfer function, H(ω), between two antennas should be measured. Using H(ω), the group delay of system can be caculated. As, it's discussed above, group delay shows the total phase distortion of an antenna. So, the dispersion of the transmitted signal can be obtained by using the group delay's information. The time that signal takes to travel from one antenna to the other is called the average group delay. These days, simulation tools are able to calculate the phase response of two antennas [84], [85]. However, this process is time consuming and needs large capacities to solve. It should be stated that there is not any specific standard for this characterization method, in order to show the acceptable delay of an UWB system. Thus, it cempletely depend on the designer's opinion to decide whether the delay is acceptable or not.

To show the simulation of group delay, CST Microwave studio and Ansoft HFSS simulation tools used to simulate a two antenna systems composed of two circular monopoles and two Vivaldi antennas [85]. Figure 3.10 shows the simulation structure which antennas are located at distance of 150 mm from each other. A MATLAB code is used to transform the phase response of the system to group delay [86]. It is worthy

to notice that simulation tools along with computer resources are playing vital role in this kind of simulation. For example, in the aforementioned simulation, also the computational time was considerably large (> 30 min) for each system, but HFSS can only handle the simulation over 150mm while CST can support a distance of 750mm.

3.1.7. Effective length, effective width, resonant frequency

Fringing effects leads to lengthening of L and widening of W (Figure 3.11). The dimensions of the patch along its length have now been extended on each end by a distance ΔL, which is a function of ε$_{reff}$ and W/h (Width-to-Height Ratio). It is given as:

$$\Delta L = 0.412h \frac{(\varepsilon_{reff}+0.3)\left(\frac{W}{h}+0.264\right)}{(\varepsilon_{reff}-0.258)\left(\frac{W}{h}+0.8\right)} \qquad (3.18)$$

Now the effective length of the patch becomes:

$$L_{eff} = L + 2\Delta L \qquad (3.19)$$

For a given resonant frequency, the effective length is given by:

$$L_{eff} = \frac{c}{2f_0\sqrt{\varepsilon_{reff}}} \qquad (3.20)$$

The resonant frequency for any rectangular microstrip patch is given as:

$$f_0 = \frac{c}{2\sqrt{\varepsilon_{reff}}}\left[\left(\frac{m}{L}\right)^2 + \left(\frac{n}{W}\right)^2\right]^{\frac{1}{2}} \qquad (3.21)$$

Where m,n are the modes for L and W respectively.

For efficient radiation the width (W) is given by:

$$W = \frac{c}{2f_0\sqrt{\frac{\varepsilon_r+1}{2}}} \qquad (3.22)$$

Where f_0 is the resonant frequency and c stands for speed of light in free space.

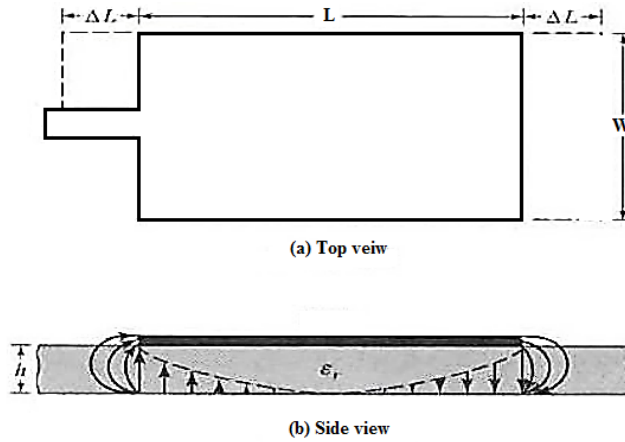(a) Top veiw

(b) Side view

Figure 3.11 : Actual and effective length of rectangular patch.

3.1.8. Bandwidth

Bandwidth increases as the substrate thickness (h) increases. In other words, the bandwidth is directly proportional to (h), if surface wave losses are ignored. However, this icreasement in substrate thickness (h) decreases the Quality factor (Q) of the cavity. This phenamenan, increases spurious radiation from the feed, and excites higher order modes in the cavity. And higher order modes lead to cross-polarization. Also, the patch becomes difficult to match as the substrate thickness increases beyond a particular point (typically about 0.05 λ_0). However, in recent years considerable effort has been done to improve the bandwidth of the microstrip antenna by using alternative feeding schemes.

The aperture coupled feed is one method that overcomes the problem of probe inductance, but it increases complexity. Decreasing the substrate permittivity also increases the bandwidth (BW) of the microstrip antenna. However, this makes the patch larger. By using a combination of aperture coupled feeding and a low permittivity foam substrate, bandwidth can be improved. The use of stacked patches can also be used to increase bandwidth even further. Formula for the bandwidth (defined by VSWR < 2.0) is,

$$BW = \frac{1}{\sqrt{2}}\left[\tan \delta_d + \left(\frac{R_s}{\pi \eta_0 \mu_r}\right)\left(\frac{1}{h/\lambda_0}\right) + \left(\frac{16}{3}\right)\left(\frac{pc_1}{\varepsilon_r}\right)\left(\frac{h}{\lambda_0}\right)\left(\frac{W}{L}\right)\left(\frac{1}{e_r^{sw}}\right)\right] \quad (3.23)$$

3.2. Feeding Techniques

After talking about different methods of characterizing an Ultra Wideband antenna, it's time to discuss different methods and techniques of feeding microstrip antennas. Variety of methods introduced to fed Microstrip patch antennas so far. These methods can be classified into two main categories;

a) Contacting feed.

b) Non contacting feed.

In the contacting method, the RF power is fed directly to the radiating patch using a connecting element such as a microstrip line or Coaxial Cable.

In the non contacting scheme, Coupling technique is used to transfer electromagnetic field power from microstrip line to the radiating patch such as aperture coupling and proximity coupling.

3.2.1 Microstrip line feed

In this technique, feeding is done by employing a conducting strip line which is connected directly to the edge of the patch. The conducting strip width would be selected according to the required impedance and it is usually smaller as compared to the patch. Noticeable advantage of this method is the ability of etching the feed line with the patch on the same substrate to provide a planar structure. Figure 3.12 shows the structure.
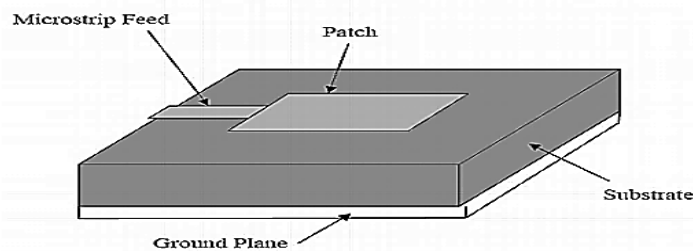

Figure 3.12 : Microstrip line feed.

Cahractrizations of this line can be found in any microwave refrence book. Here, we only represent the calculation of impedance as an important part of antenna design. By assuming a substrate with the height of h for a given width of microstip line, the characteristic impedance of a the line can be calculated as

$$
Z_0 = \begin{cases}
\dfrac{60}{\sqrt{\varepsilon_e}} \ln\left(\dfrac{8h}{w} + \dfrac{w}{4h} \right) & for\ \dfrac{w}{h} \le 1 \\[6mm]
\dfrac{120\pi}{\sqrt{\varepsilon_e}\left[\dfrac{w}{h} + 1.393 + 0.667 \ln\left(\dfrac{w}{h} + 1.444 \right) \right]} & for\ \dfrac{w}{h} \ge 1
\end{cases}
$$

(3.24)

Where ε_e is defined as an effective dielectric constant and can be calculated as:

$$
\varepsilon_e = \frac{\varepsilon_r + 1}{2} + \frac{\varepsilon_r - 1}{2} \left(\frac{1}{\sqrt{1 + \dfrac{12h}{w}}} \right)
$$

(3.25)

According to these equations, the width of feeding line can be selected to provide 50Ω and gave a good impedance matching.

3.2.2 Coaxial feed

The coaxial feed or probe feed is the other feeding method for Microstrip antennas. As it is shown in Figure 3.13, the inner conductor of the coaxial connector extends through the dielectric and is attached to the radiating patch, while the outer conductor is connected to the ground plane.

Using this technique enables the designer to place the feed at any desired location inside the patch in order to match with its input impedance. This method is easy to fabricate and has low spurious radiation. On the other hand, narrow bandwidth of this feeding method is its main disadvantage. It is also difficult to model since a hole has to be made in the substrate and the connector lumps outside the ground plane.
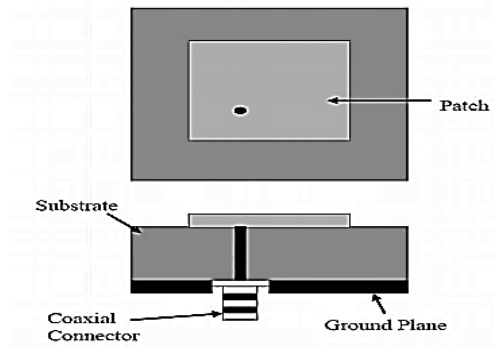
Figure 3.13 : Probe fed rectangular microstrip patch antenna.

3.2.3. Aperture coupled feed

The aperture coupling method is the other commonly used technique which has a lot of difficulties in fabrication. This method is very easier to model and has little spurious radiation problem. As, it's illustrated in Figure 3.14, in this feeding technique, ground plane will take place between patch and feeding line with a slot on it. The electrmagnetic energy will couple between the feed line and patch through this slot. The amount of coupling energy, from the feed to the patch, depends on the shape, size and location of the aperture. In most of the structures, the coupling aperture would be located under the patch to provide lower cross polarization. spurious radiation is in its minimum value while using this method because, the ground plane separates the patch and the feed. Generally, the top substrate is thick with low dielectric constant and the bottom substrate consists of a high dielectric material to optimize radiation from the patch.

As mentioned, main disadvantage of this technique is its difficulty in fabrication process due to presence of multiple layers. This feeding scheme also produces narrow bandwidth.
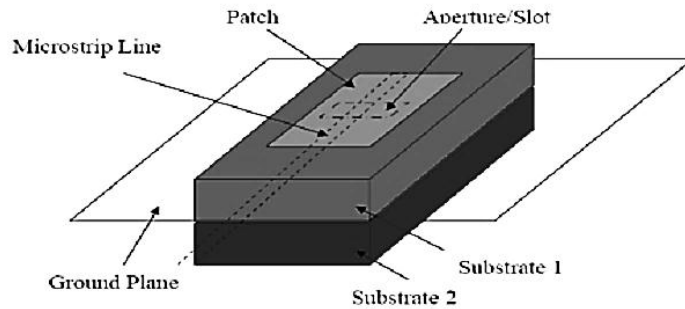
Figure 3.14 : Aperture coupled feed.

3.2.4. Proximity coupled feed

This feed technique employs electromagnetic coupling scheme. Again, as the aperture coupling feed, two dielectric substrates are used. The patch placed on top of the structure and the bottom of it is ground plane. Feed line is located between the two substrates (Figure 3.15).

Minimum spurious feed radiation is the main advantage of this method. This method also offers high bandwidth (as high as 13%), due to overall increasement of in the thickness of the antenna. This method gives the designer more options by selecting dielectric materials for both substrates; so, designer has more choice to optimize the individual performances.
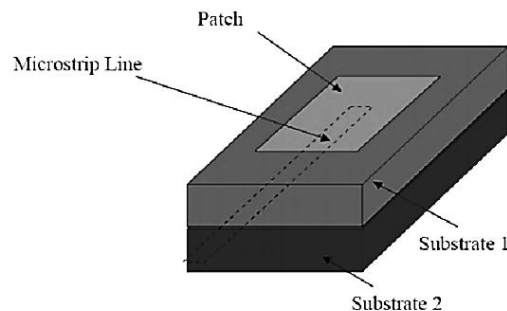
Figure 3.15 : Proximity coupled feed.

Again, manufacturing difficulties is the major disadvantage of this feeding method, because of the required alignment between two dielectric layers.

4. DESIGN OF NEW UWB MICROSTRIP ANTENNA

The geometries of the antennas in this thesis are determined by implementing parametric studies using Ansoft HFSS. The software is an electromagnetic structure's solver, based on Finite Element Method (FEM) [87]. HFSS is known as one of the popular commercial tools useing for antenna design, and complex RF electronic circuit elements such as transmission lines and filters.One of the outstanding feature of this software (HFSS) is automated solution process. This means that, it's only needed to specify the geometry, material properties and the desired outputs. The software will automatically generate the appropriate mesh for solving the problem. Presenting work is based on previous works in this field. Detailed parametric study of the antenna will be discussed as follows.

4.1. A New UWB Microstrip Antenna Using Coaxial Probe Feeding

Following sections present details of the new design to increse bandwidth in order to achieve the UWB frequency range and parametric study of the new antenna characters.

4.1.1. Antenna design

The proposed Heptagon UWB antenna geometry and its dimensions are presented in Figure 4.1. This antenna is printed on a 30mm×30mm FR4 substrate with the thickness of 4mm and relatively permittivity of 4.4. The antenna ground is uniform, without any defected part. The antenna is fed by using probe fed technique.

Table 4.1 provides parameters of antenna and final achieved values of each parameter.

Table 4. 1 : Physical parameters of the antenna and final dimensions

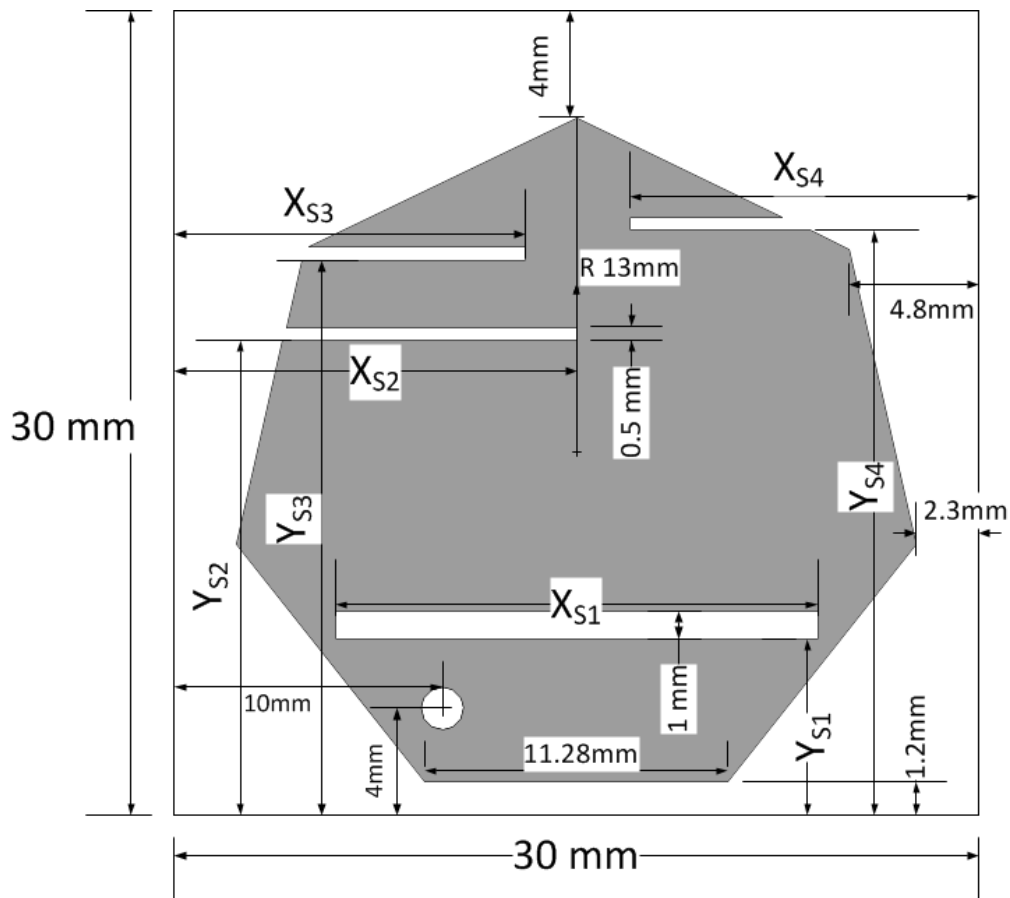| Parameters	Dimensions (mm)
Total size	30mm × 30mm
Radius	13 mm
X_{S1}	18 mm
X_{S2}	15.5 mm
X_{S3}	9.1 mm
X_{S4}	14 mm
Y_{S1}	6.6 mm
Y_{S2}	16.7 mm
Y_{S3}	20.7 mm
Y_{S4}	22.3 mm

Figure 4.1 : Geometry of the proposed antenna.

4.1.1.1. Study of the effects of shape and feed location

The introduced geometry has been selected by performing parametric analysis. Main parameters in this design are shape of the patch and location of the coax feeding. Fig. 4.2 presents different positions of feeding that had been tested. It also represents current passes for each position.
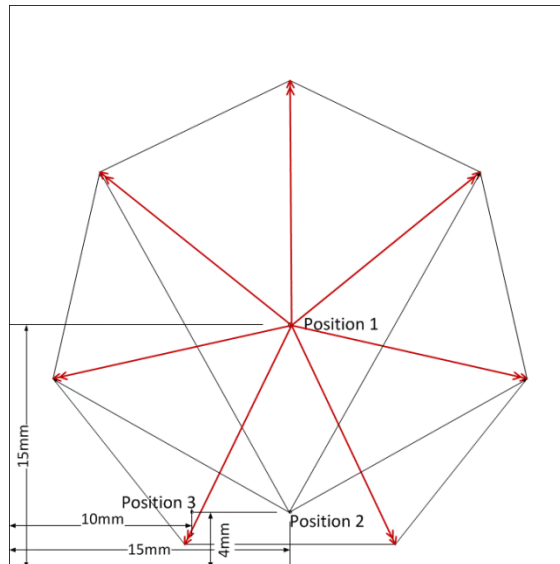
Figure 4.2 : Different positions of feeding and current routs.

Location of the feed can be selected according to this fact that electrical length of antenna will determine the resonant frequency. Placing the feed in the center of the patch brings us almost equal lengths of surface current, see Fig. 4.2. Fig. 4.3 to Fig. 4.4 shows the study of different shapes for patch with every three assumed position of feed. As it's shown in Fig. 4.3, we will achieve less than one gigahertz bandwidth around the resonant frequency of 7.2 GHz. In next step, feed moved to the side of patch which causes different length for the current. As it's illustrated in Fig. 4.4, there are still routes with the same length and so, it didn't result in a broad bandwidth. Thus, feed moved to a corner to imply different passes of current flow in the patch. Using this location for feed and shape of heptagon for patch, gave three resonant frequencies in 5.75GHz, 8.25GHz and 9.6GHz. Simulation result of $|S_{11}|$ for this location of feed is shown in Fig. 4.5. As it is clear, shape of heptagon and feed in a corner, provides better $|S_{11}|$ in comparison with the others.
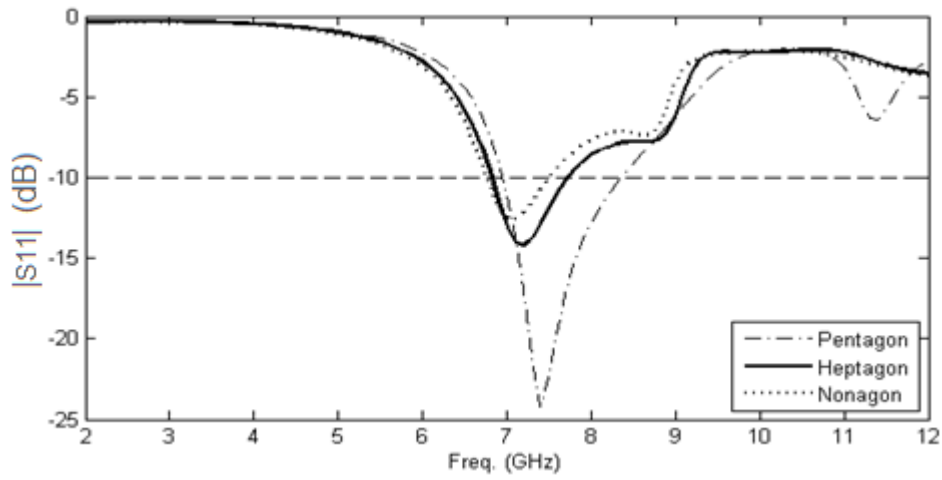
Figure 4.3 : $|S_{11}|$ for different shapes of patch with the feed located in position 1.
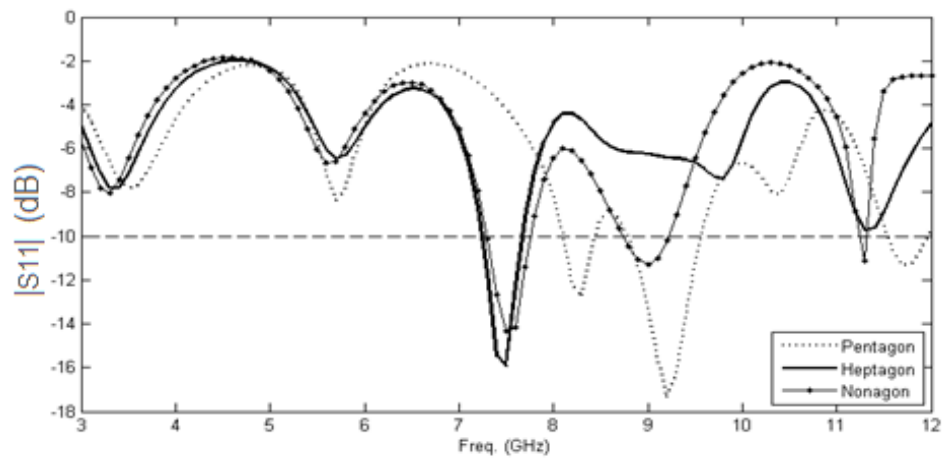

Figure 4.4 : $|S_{11}|$ for different shapes of patch with the feed located in position 2.
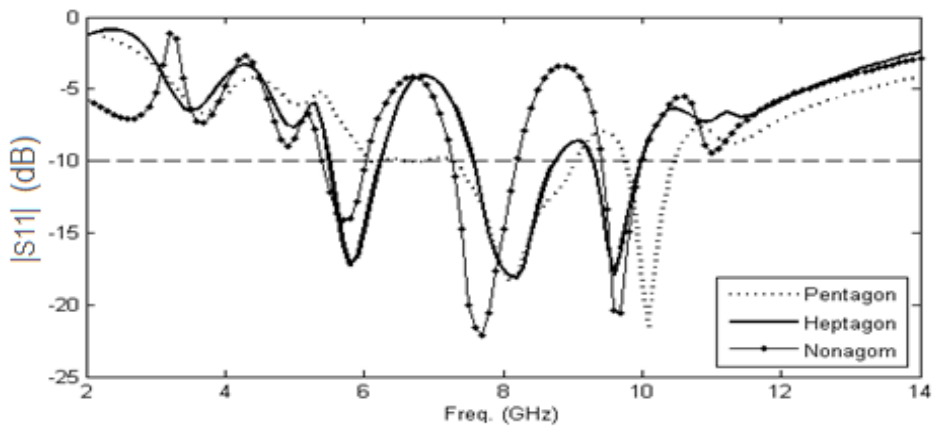

Figure 4.5 : $|S_{11}|$ for different shapes of patch while locating the feed in position 3.

4.1.1.2 Effects of S1

By reconsidering the aforementioned idea as a basic theory, it's been decided to use slots, in order to control current passes in a desired rout with more accuracy. Slot, named S1, placed near the feed location which results two different passes for surface current with various lengths. Implementing this slot increases bandwidth around the resonant frequencies, also there is a slight shift in resonant frequencies. Fig. 4.6 shows $|S_{11}|$ result using this slot. Surface currents for both structures, with and without slot of S1, presented in Fig 4.7, which simply clarifies the result of $|S_{11}|$.
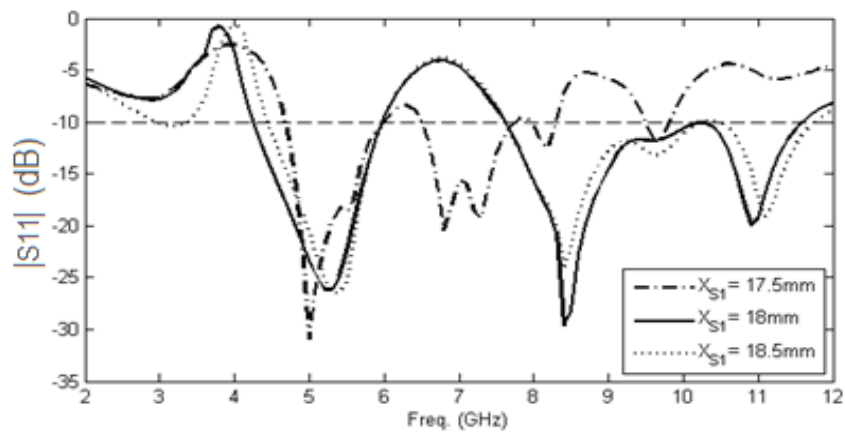
(a)
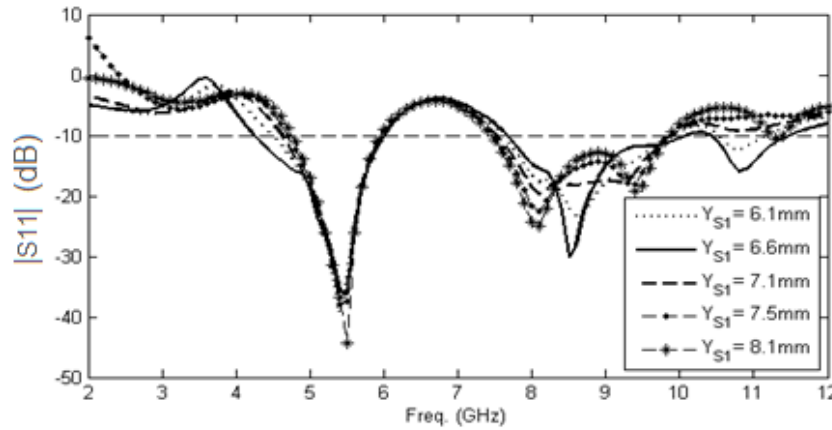
(b)

Figure 4.6 : The effect of S1 while feed is in positin 3. (a) Length of S1 (Y_{S1}=6.6mm), (b) Position of S1 (X_{S1}=18mm).
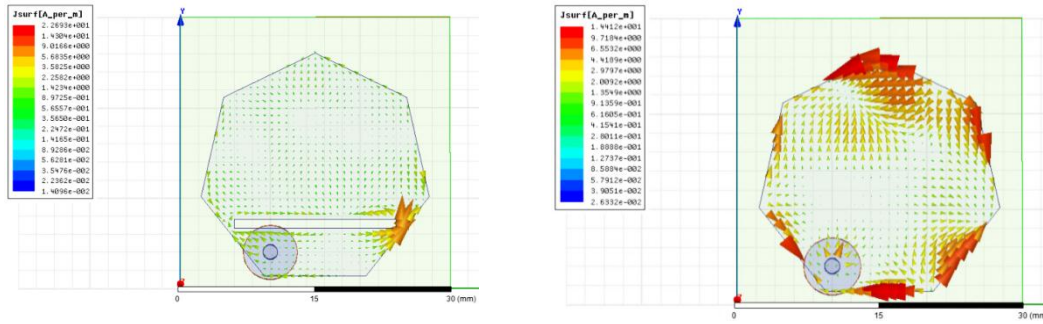
Figure 4.7 : Surface currents and the effect of S1.

4.1.1.3. Effects of S2

By monitoring the surface current on the patch in different frequencies, it's determined that there is a need for another slot to control the path of the current. This slot which is shown as S2 in Figure 4.1, helps us in eliminating the notch between 6-8 GHz. Figure 4.8 shows parametric analysis for different positions of S2 to indicate the optimum location. Furthermore, the parametric study of the length of this slot is shown in Figure 4.9 and the optimum length of 15.5mm is selected.
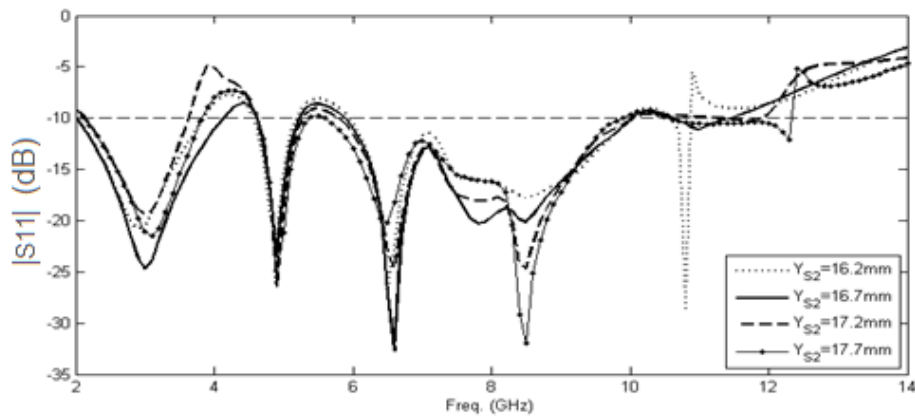

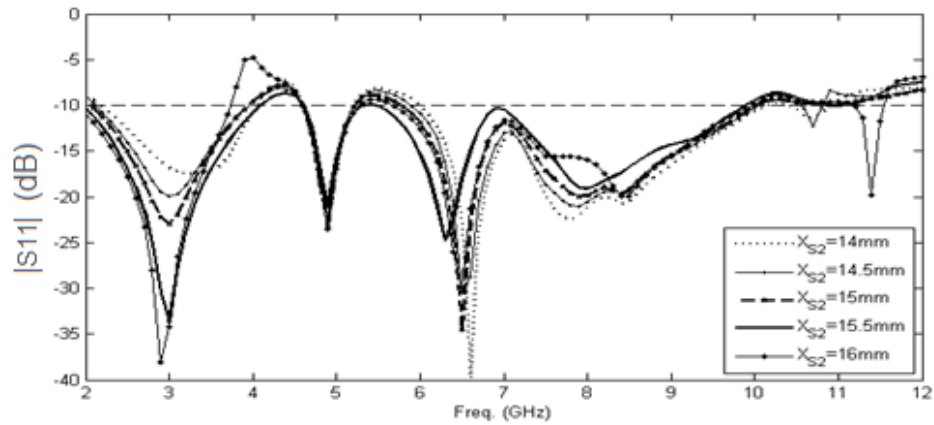**Figure 4.8 :** $|S_{11}|$ for different positions of S2 (X_{S2}=15.5mm).

Figure 4.9 : $|S_{11}|$ for different lengths of S2 (Y_{S2}=16.7mm).

Surface current of the proposed patch with the slots S1 and S2 in various frequencies is shown in Figure 4.10 to clarify the passes of the current and achieved reason.
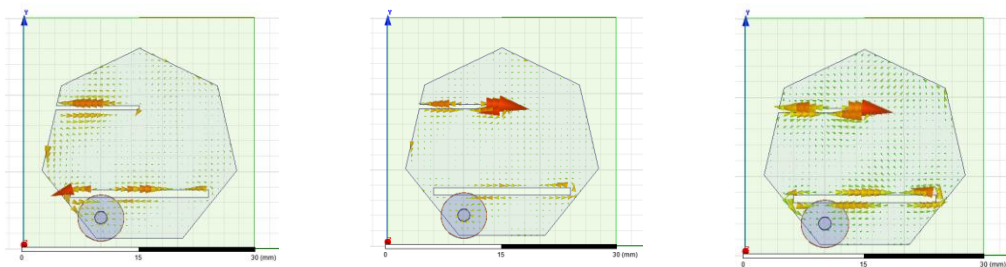

Figure 4.10 : Surface currents of three resonant frequencies with S1 and S2.

4.1.1.4. Effects of S3

In the next step, a slot named S3 added to improve the results of the $|S_{11}|$ for proposed antenna. Figure 4.11 and 4.12 shows parametric analysis of the length and position of this slot. As it's illustrated in Figure 4.11, adding this slot will help to control the band notch around 4GHz and able us to reach the bandwidth of 2GHz to 9.6GHz.
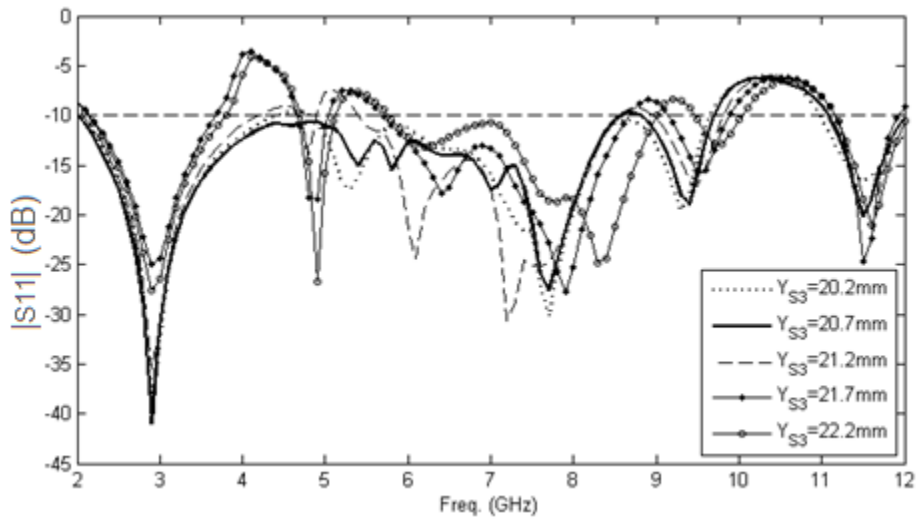
Figure 4.11 : $|S_{11}|$ for different values of S3's position (X_{S3}=9.1mm).
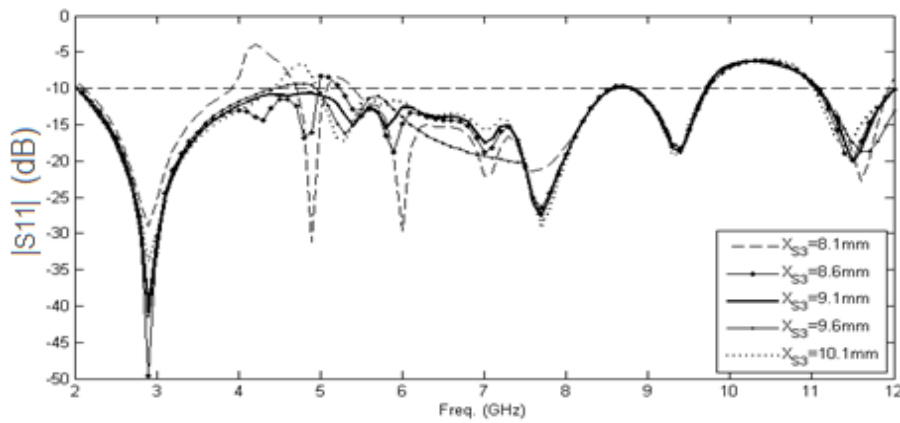
Figure 4.12 : $|S_{11}|$ for various lengths of S3 (Y_{S3}=21.2mm).

4.1.1.5. Effects of S4

A good bandwidth using step by step moving forward achieved so far. But, according to the definition of UWB, 3.1GHz to 10.6GHz need to be covered. In order to reach this frequency range, another slot had been implemented, shown as S4. As it's illustrated in Figures 4.13 and 4.14, by preforming parametric analysis on the position of this slot, optimum point reached.

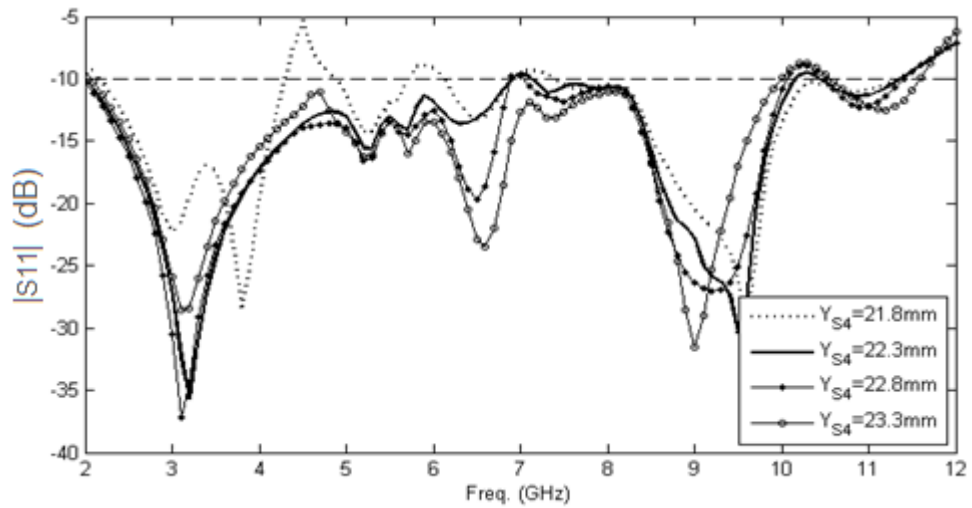**Figure 4.13 :** $|S_{11}|$ for different positions of S4 (X_{S4}=14mm).
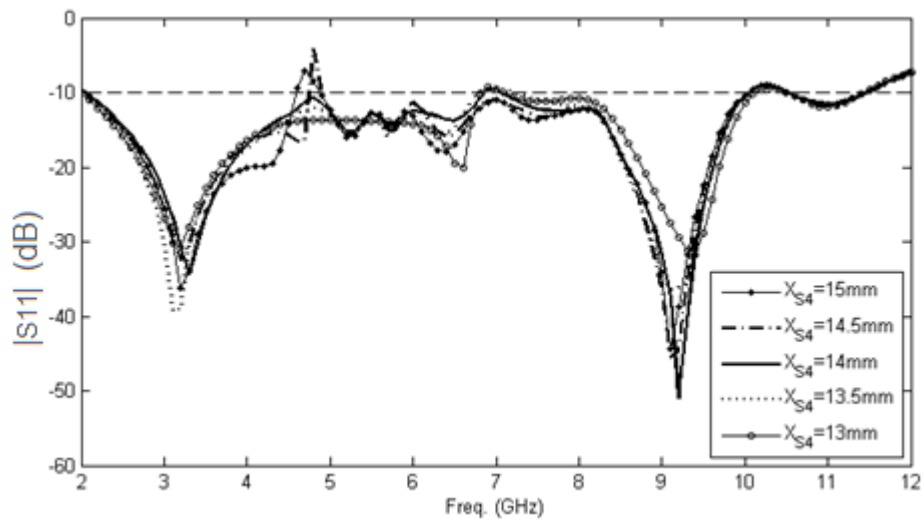
Figure 4.14 : $|S_{11}|$ for different lengths of S4 (Y_{S4}=22.3mm).

4.1.1.6. Fabrication and test

To validate the results of simulation, the proposed antenna has been fabricated and tested.

4.1.1.6.1. Radiation pattern

As it's discussed, due to UWB applications, there is demand for omnidirectional radiation pattern. Figure 4.15 shows the radiation pattern of proposed antenna. It's clear that because of the uniform ground plane, radiation pattern has no back lob, but still keeps its omnidirectional shape.
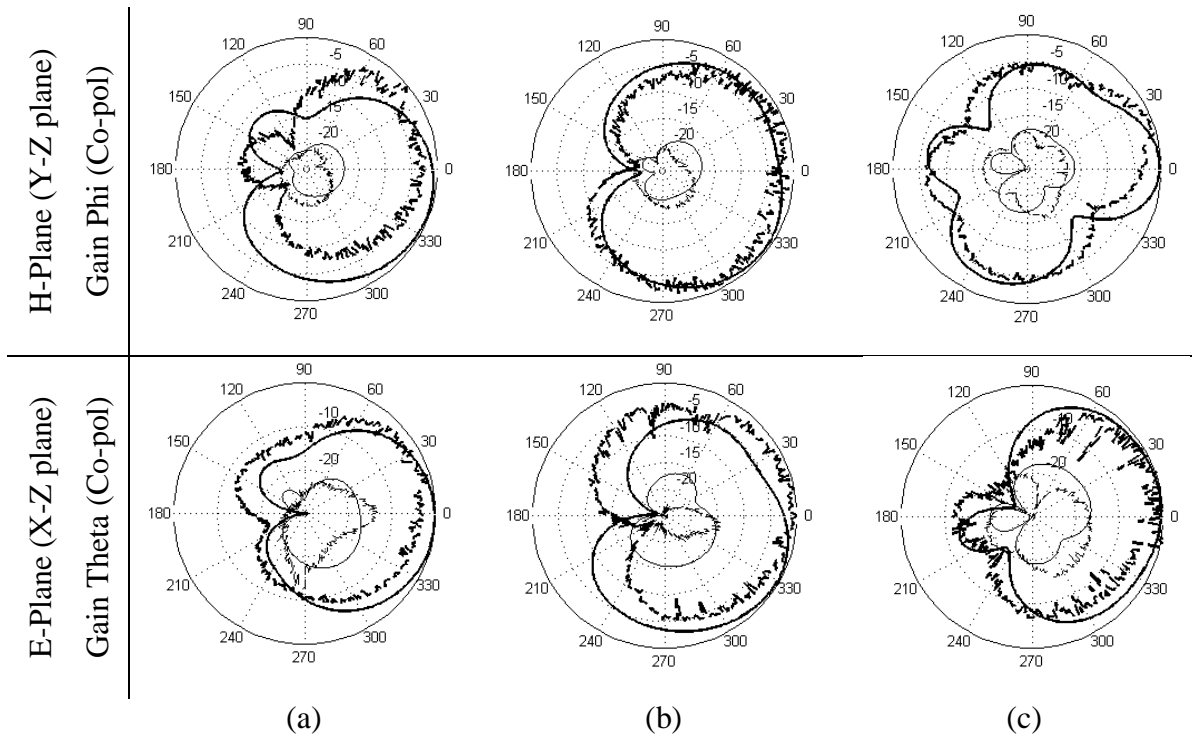
Figure 4.15 : Normalized radiation gain patterns of the proposed antenna. (—) Simulated. (⋯) Measured. (a) 4GHz, (b) 6GHz, (c) 8GHz.
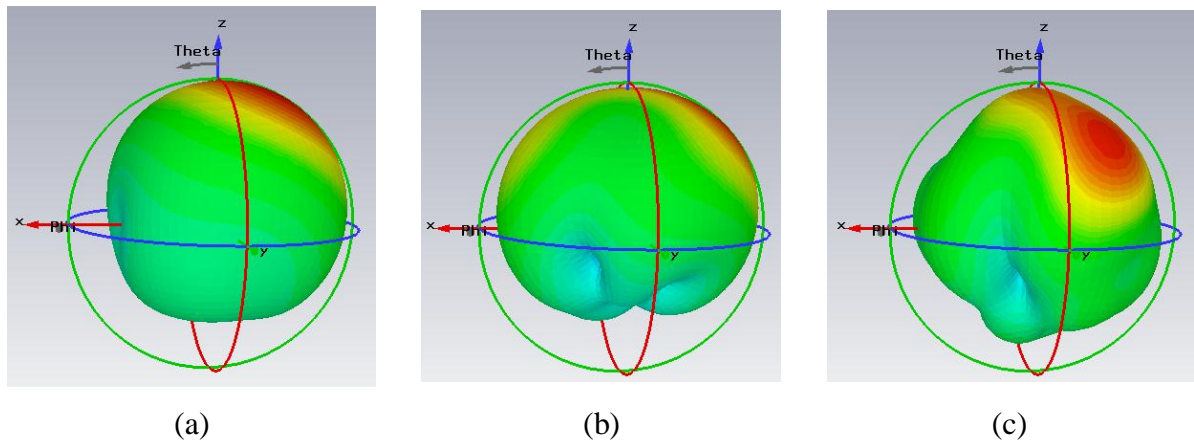
Figure 4.16 : 3D gain pattern in (a) 4GHz, (b) 6GHz, (c) 8GHz.

Figure 4.16 shows 3D gain pattern in mentioned frequencies.

Figure 4.17 provides the gain of proposed antenna vs. frequency. In the proposed structure, the height of substrate reduces the antenna gain. But still it's acceptable for all known applications of UWB.

It also should be mentioned that, the according to the co and cross patterns of the proposed antenna, the polarization is linear (vertical).

46
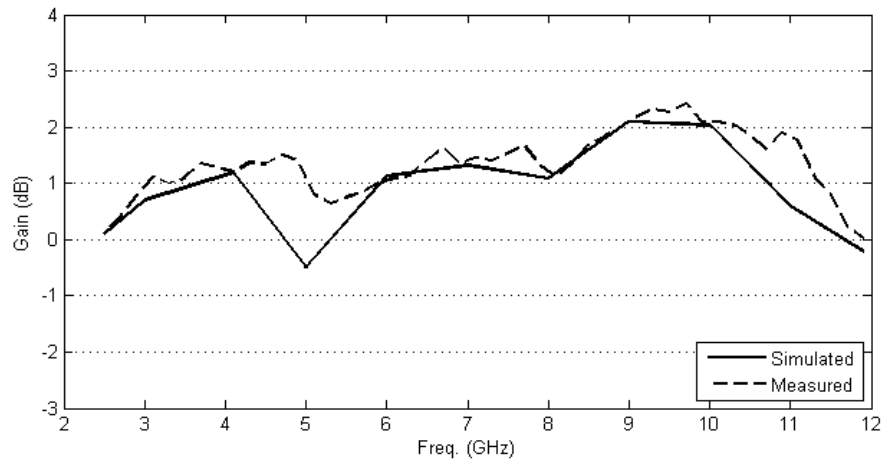
Figure 4.17 : Gain of the antenna at θ=0, φ=0.
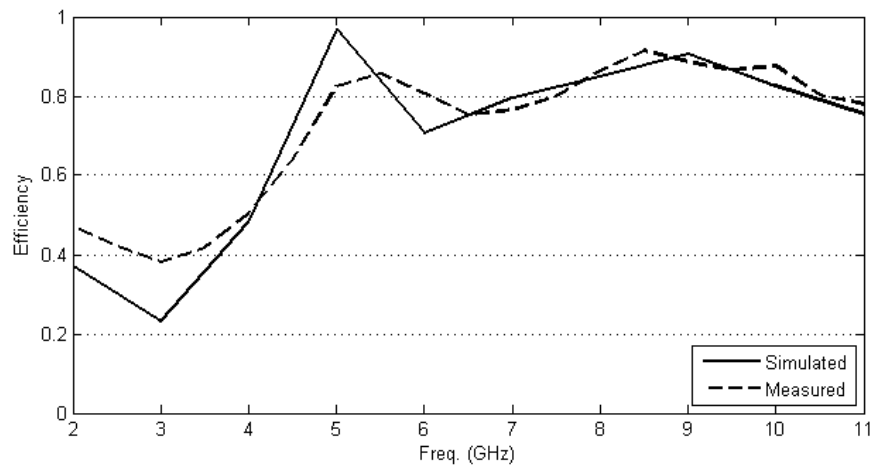
Figure 4.18 : Efficiency of the proposed antenna.

Figure 4.18 presents the efficiency of the proposed antenna which indicates acceptable efficiency in UWB band range.

4.1.1.6.2. Group delay

Figure 4.19 shows the group delay diagram for all the available UWB frequencies. It's clear that, delay of this antenna is less than 2 ns which will provide a good communication state for different applications.
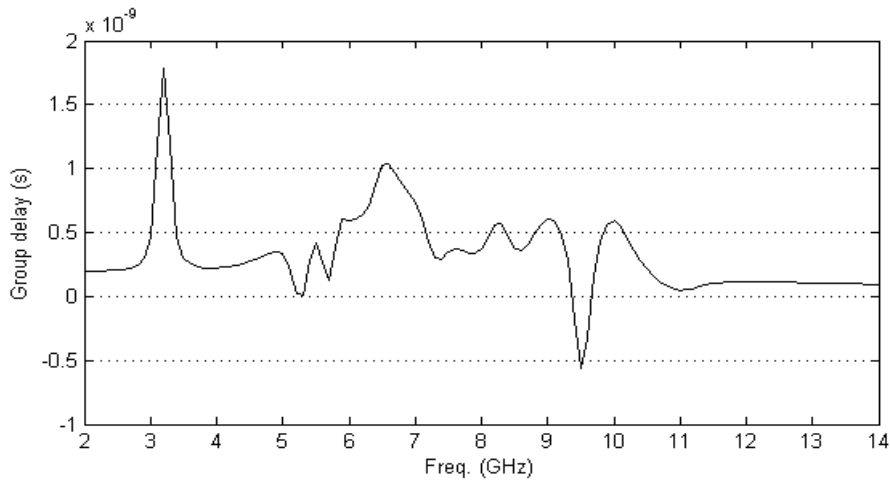
Figure 4.19: Measured group delay of proposed antenna.

Figure 4.20 shows the fabricated antenna. Figure 4.21 provides measurement results in comparison with the simulated $|S_{11}|$ of the antenna. The tests had been done using Agilent Technologies E8363C PNA network analyzer. Results show that fabricated antenna works well and provides the desired UWB bandwidth. However, there are mismatches because of fabrication process.
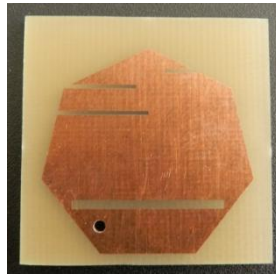
Figure 4.20 : Fabricated antenna.
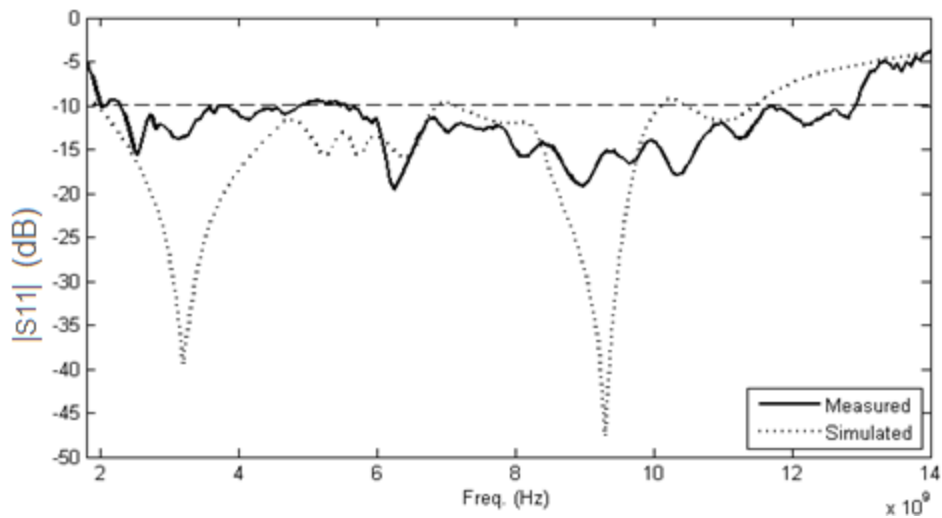
Figure 4.21 : Simulated and measured $|S_{11}|$ of proposed antenna.

48

Table 4.2 presents a comparison between the proposed antenna and results of some previous presented works.

Table 4.2 A comparison the proposed antenna with the results of [33], [34] and [35].

	Proposed antenna in the thesis	Proposed antenna in [33]	Proposed antenna in [34]	Proposed antenna in [35]
Size	30mm × 30mm	67mm × 74mm	50mm × 50mm	21.4mm × 4.5mm
Bandwidth	2.2 – 11.5 GHz	5.17 - 5.81 GHz	3.87 - 13.46 GHz	10.3 – 17.9 GHz
Substrate	FR4 (ε_r= 4.4)	Rogers RT\Duroid (ε_r= 2.2)	ε_r= 1	ε_r= 2.1 and ε_r= 1
Thickness	4mm	3.175mm	7mm	4mm
Max. Gain	4.39 dB (φ= 220, θ=20)	8.11 dBi	6 dBi	7.53 dB

5. CONCLUSION AND RECOMMENDATIONS

The major purpose of this research was to achieve the two hypotheses mentioned in the first section. In this section, an overview of the work has been presented. A review study of previous works done and different techniques in widening bandwidth studied. In the second chapter, it's tried to completely clarify UWB technologies, emphasizing the most important concepts in antenna design. Section three gives list of the characteristics that are using to characterize UWB antennas. In section four, a new microstrip patch antenna for UWB systems has been presented. The antenna has dimensions of 30mm×30mm which gives various usages due to its small size. The design and fabrication of the antenna has been done on a substrate of FR4 with ε_r=4.4. This feature results in low cost fabrication which seems vital in industry. Probe feeding technique has been employed in this design. In order to overcome the probe feeding limited bandwidth, different shapes had been studied to improve the bandwidth. Finally, a heptagon shape patch chose as a proper shape. Slots have been employed to enhance the bandwidth. Bringing together all these techniques, an UWB frequency range has been achieved. All the simulations have been done using HFSS software.

Suggestions for future works:

1- Investigating other feeding techniques such as aperture coupling in order to achieve better characteristics.

2- Investigating different cheap substrates or multilayer substrates and shapes to decrease the overall height of the antenna.

3- Employ some very new materials such as meta-materials in order to improve bandwidth and other characteristics.

REFERENCES

[1] **P.S.Hall, C.Wood, c.Garrett**, 1970: Wide bandwidth micro strip antennas for circuit integration. IEE Electron. Lett., vo1.1S, pp. 458-460.

[2] **C.Wood**, 1980: Improved bandwidth of microstrip antenna using parasitic elements. IEE Proc., Pt.H, vol. 127, pp.231-234.

[3] **A.G.Derneryd and LKarlsson**, 1981: Broad band microstrip antenna element and array. Antennas and Propagation, IEEE Transactions on, vol. AP-24, pp. 140-141.

[4] **N.Das and J.Chatterjee**, 1983: Conically depressed microstrip patch antenna. lEE Proc., Pt.H, vo1.l30, pp.193-196.

[5] **A.Saban**, May 1983: A new broadband stacked two layer antenna. Dig. Int. Symp. Antennas and Propagat., vol.l, pp.63-66.

[6] P.**S.Bhatnagar, J.P. Daniel, K.Mahadjoubi and C.Terret**, 1985: Experimental study on stacked microstrip Antennas. lEE Electron. Lett., vol.22, 864-865.

[7] **M.Deepukann J.George, C.K.Anandan, P.Mohanan and K.G.Nair**, 1996: Broadband dual frequency microstrip antenna. IEEE Electron. Lett., vo1.32, No.I7, pp. 1442-1443.

[8] **K.M Luck, K.F.Lee and Y.L.Chow**, 1998: Proximity coupled stacked circular disc microstrip antenna with slots. lEE Electron. Lett., vo1.34, no.5, pp. 419-420.

[9] **K.M Luk, C.L.Mak, Y.L Chow and K.F Lee**, 1998: Broadband microstrip patch antenna. lEE Electron. Lett., vol.34, no.15 pp. 1442-1443.

[10] **Y.x.Guo, K.M.Luk and K.F.Lee**, 1999: U-slot circular patch antenna with L probe. IEE Electron. Lett., vo1.35, no.20, pp. 1694-1695.

[11] **Kin-Lu Wong, Saou-Wen Su, and Chia-Lun Tang,** January 2005: Broadband Omnidirectional Metal-Plate Monopole Antenna. IEEE transactions on antennas and propagation, vol. 53, no. 1.

[12] **W. L. Stutzman and G. A. Thiele**, 1998: Antenna Theory and Design, 2nded. New York: Wiley, p. 172.

[13] **S.-Y. Suh and W. L. Stutzman**, 2000: A Planar Inverted Cone Antenna. http://www.vtip.org/Licensing/disclosures/00-130.htm.

[14] **S.-Y. Suh**, July 2002: A comprehensive investigation of new planar wideband antennas. Ph.D. dissertation, Virginia Polytech. Inst. State Univ., Blacksburg, VA.

[15] **Kawakami, H., and Sato, G.**, 1987: Broadband characteristics of rotationally symmetric antennas and thin wire constructs. Antennas and Propagation, IEEE Transactions on, 35, pp. 26-32.

[16] **Nakano, H., lkeda, N., Wu, Y., Suzuki, R., Mimaki, H., and Yamauchi, J.**, 1998: Realization of dual-frequency and wide-band VSWR performances using normal helical and inverted-F antennas. Antennas and Propagation, IEEE Transactions on, 46, pp. 788-793.

[17] **Rogers, S.D., and Butler, C.M.**, 2000: Cage antennas optimised for bandwidth. Electron. Lett. 36, (11), pp. 932-933.

[18] **Cho,W., Kanda,M., Hwang, H., and Howard,M.W.**, 2000: A disk-loaded thick cylindrical dipole antenna for validation of an EMC test site from 30 to 300 MHz Electromagnetic Compatibility, IEEE Transactions on, 42, pp. 172-180.

[19] **Brown, G.H., and Woodward, O.M.,** 1952: Experimentally determined radiation characteristics of conical and triangular antennas. RCA Rev., 13, (4), pp. 425-452.

[20] **M. J. Ammann and Z. N. Chen**, April 2003: A wide-band shorted planar monopole with bevel. Antennas and Propagation, IEEE Transactions on, vol. 51, no. 4, pp. 901-903.

[21] **Agrawall, N.P., Kumar, G., and Ray, K.P.,** 1998: Wide-band planar monopo1e antenna. Antennas and Propagation, IEEE Transactions on, 46, pp.294-295.

[22] **Ammann, MJ,** 1999: Square planar monopole antenna. Presented at National Conf. Antennas & Propag., York, England, pp. 37-40.

[23] **Chen, Z.N.**, 2002: Impedance characteristics of planar bow-tie-like monopole antennas. Electron. Lett. 36, (13), pp. 1100-1101.

[24] **J. Michael Lohnson and Yahya Rahmat-Samii,** 1999: The Tab Monopole. Antennas and Propagation, IEEE Transactions on, 45, pp. 187-188.

[25] **S. Honda, M. Ito, H. Seki, and Y. linbo**, 1992: A disc monopole antenna with 1:8 impedance bandwidth and omnidirectional radiation pattern. In Proc.Int. Symp. Antennas Propagation, Sapporo, Japan, pp. 1145-1148.

[26] **M. Hammoud, P. Poey, and F. Colombel**, February 1993: Matching the input impedance of a broadband disc monopole. Electron. Lett., vol. 29, pp. 406-407.

[27] **N. P. Agrawall, G. Kumar, and K. P. Ray**, February 1998: Wide-band planar monopole antennas. Antennas and Propagation, IEEE Transactions on, vol. 46, pp. 294-295.

[28] **P. V. Anob, K. P. Ray, and G. Kumar**, July 2001: Wideband orthogonal square monopole antennas with semi-circular base. In Proc. IEEE Antennas Propagat. Soc. Int. Symp. Dig., vol. 3, Boston, MA, pp.294-297.

[29] **M. J. Ammann**, August 2001: Control of the impedance bandwidth of wideband planar monopole antennas using a bevelling technique. Microwave Opt. Technol. Lett., vol. 30, pp. 229-232.

[30] **M. 1. Ammann and Z. N. Chen**, April 2003: Wideband monopole antennas for multi-band wireless systems. IEEE Antennas Propagat. Mag., vol. 45, pp. 146-150.

[31] **S.-Y. Suh, W. L. Stutzman, and W. A. Davis**, Multi-broadband monopole disc antennas. In Proc. IEEE Antenna & Propagation Soc. Int. Symp. Dig., vol. 3, Columbus, OH, pp. 616-619.

[32] **E. Antonino-Daviu, M. Cabedo-Fabres, M. Ferrando-Bataller, and A. Valero-Nogueira**, November 2003: Wideband double-fed planar monopole antennas. Electron. Lett. vol. 39, pp. 1635-1636.

[33] **Khidre, A; Kai-Fong Lee; Elsherbeni, AZ.; Fan Yang**, March 2013: Wide Band Dual-Beam U-Slot Microstrip Antenna. *Antennas and Propagation, IEEE Transactions on* , vol.61, no.3, pp.1415,1418.

[34] **Malekpoor H. and Jam S.,** 2012: Ultra-wideband fed by folded-patch with multi resonances shorted patch antennas. Progress In Electromagnetics Research B, Vol. 44, 309–326.

[35] **Ghassemi, N.; Neshati, M.H.; Rashed-Mohassel, J.**, December 2007: Investigation of Multilayer Probe-Fed Microstrip Antenna for Ultra Wideband Operation. *Microwave Conference, 2007. APMC 2007. Asia-Pacific* , vol., no., pp.1,4, 11-14.

[36] **Ghannoum, H.; Bories, S.; Roblin, C.**, September 2005: Probe fed stacked patch antenna for UWB. *Ultra-Wideband, 2005. ICU 2005. 2005 IEEE International Conference on* , vol., no., pp.97,102, 5-8.

[37] **A Eldek, A.Z Elsherbeni and C.E Smith**, 2005: Rectangular Slot Antennawith Patch stub for Ultra Wideband Applications and Phased ArraySystems. PIER 3,pp. 227-237.

[38] **Ashwini K. Arya, M. V. Kartikeyan, A .Patnaik**, October 2010: Defected Ground Structure in the perspective of Microstrip antenna. Frequency, Vol.64, Issue5-6, pp.79-84.

[39] **Zheng Guo; Huiping Tian; Xudong Wang; Qun Luo; Yuefeng Ji**, 2013: Bandwidth Enhancement of Monopole UWB Antenna With New Slots and EBG Structures. Antennas and Wireless Propagation Letters, *IEEE* , vol.12, no., pp.1550,1553.

[40] **WiMedia Alliance**. [Online]. Available: http://www.wimedia.org/en/index.asp

[41] **M. Z. Win and R. A. Scholtz**, February 1998: Impulse radio: how it works. IEEE Commun. Lett., vol. 2, no. 2, pp. 36-38.

[42] **F. J. Agee, C. E. Baum, W. D. Prather, J. M. Lehr, J. P. O'Loughlin, J. W. Burger, J. S. H. Schoenberg, D. W. Scholeld, R. J. Torres, J. P. Hull, and J. A. Gaudet**, Jun. 1998: Ultrawideband transmitter research. IEEE Trans. Plasma Sci., vol. 26, no. 3, pp. 860-873.

[43] **W. D. Prather, C. E. Baum, J. M. Lehr, J. P. O'Loughlin, S. Tyo, J. S. H. Schoenberg, R. J. Torres, T. C. Tran, D. W. Scholeld, J. Gaudet, and J. W. Burger**, October 2000: Ultra-wideband source and antenna research. IEEE Trans. Plasma Sci., vol. 28, no. 5, pp. 1624-1630.

[44] **D. M. Pozar**, December 2007: Optimal radiated waveforms from an arbitrary UWB antenna. IEEE Trans. Antennas Propag., vol. 55, no. 12, pp. 3384-3390.

[45] **Q. Wang and J. Yao**, November 2007: An electrically switchable optical ultrawideband pulse generator. J. Lightw. Technol., vol. 25, no. 11, pp. 3626-3633.

[46] **X. Chen and S. Kiaei**, 2002: Monocycle shapes for ultra wideband system. In Proc. IEEE International Symposium on Circuits and Systems ISCAS 2002, vol. 1, May 26-29, pp. I-597-I-600.

[47] **J. Ryckaert, M. Badaroglu, C. Desset, V. De Heyn, G. ven der Plas, P. Wambacq, B. van Poucke, and S. Donnay**, 2005: Carrier-based UWB impulse radio: simplicity, exibility, and pulser implementation in 0.18-micron CMOS. In Proc. IEEE International Conference on Ultra-Wideband ICU 2005, Sep. 5-8, pp. 432-437.

[48] **R. Xu, Y. Jin, and C. Nguyen**, August 2006: Power-e-cient switching-based cmos uwb transmitters for uwb communications and radar systems. Microwave Theory and Techniques, IEEETransactions on, vol. 54, no. 8, pp. 3271 -3277.

[49] **S. Wood and R. Aiello**, 2008: Essentials of UWB, ser. Cambridge Wireless Essential Series. Cambridge University Press.

[50] **intel**. [Online]. Available: http://www.intel.com/technology/usb/.

[51] **S.-W. Su, J.-H. Chou, and K.-L. Wong**, April 2007: Internal ultrawideband monopole antenna for wireless usb dongle applications. Antennas and Propagation, IEEE Transactions on, vol. 55, no. 4, pp. 1180-1183.

[52] **D. Krishna, M. Gopikrishna, C. Aanandan, P. Mohanan, and K. Vasudevan**, 2008: Ultrawideband slot antenna for wireless usb dongle applications. Electronics Letters, vol. 44, no. 18, pp. 1057 -1058, 28.

[53] **T. G. Savelyev, L. van Kempen, H. Sahli, J. Sachs, and M. Sato**, January 2007: Investigation of time ndash;frequency features for gpr landmine discrimination. Geoscience and Remote Sensing, IEEE Transactions on, vol. 45, no. 1, pp. 118-129.

[54] **L. Carin, R. Kapoor, and C. Baum**, November 1998: Polarimetric SAR imaging of buried landmines, Geoscience and Remote Sensing, IEEE Transactions on, vol. 36, no. 6, pp. 1985-1988.

[55] **X. Li, E. Bond, B. Van Veen, and S. Hagness**, February 2005: An overview of ultra-wideband microwave imaging via space-time beamforming for early-stage breast-cancer detection. Antennas and Propagation Magazine, IEEE, vol. 47, no. 1, pp. 19 -34.

[56] **S. Salvador and G. Vecchi**, June 2009: Experimental tests of microwave breast cancer detection on phantoms. Antennas and Propagation, IEEE Transactions on, vol. 57, no. 6, pp. 1705-1712.

[57] **E. Staderini**, January 2002: UWB radars in medicine. Aerospace and Electronic Systems Magazine, IEEE, vol. 17, no. 1, pp. 13-18.

[58] **L. Jofre, A. Broquetas, J. Romeu, S. Blanch, A. Toda, X. Fabregas, and A. Cardama**, February 2009: UWB tomographic radar imaging of penetrable and impenetrable objects. Proceedings of the IEEE, vol. 97, no. 2, pp. 451 464.

[59] **M. Klemm, I. Craddock, J. Leendertz, A. Preece, and R. Benjamin**, June 2009: Radar-based breast cancer detection using a hemispherical antenna array - experimental results. Antennas and Propagation, IEEE Transactions on, vol. 57, no. 6, pp. 1692-1704.

[60] **J.-Y. Lee and R. Scholtz**, December 2002: Ranging in a dense multipath environment using an UWB radio link. Selected Areas in Communications, IEEE Journal on, vol. 20, no. 9, pp. 1677-1683.

[61] **E. Saberinia and A. Tewk**, July 2008: Ranging in multiband ultrawideband communication systems. Vehicular Technology, IEEE Transactions on, vol. 57, no. 4, pp. 2523-2530.

[62] **Y. Takeuchi, Y. Shimizu, and Y. Sanada**, June 2006: Examination of antenna combinations for uwb ranging system. Microwave Theory and Techniques, IEEE Transactions on, vol. 54, no. 4, pp. 1858-1864.

[63] **FCC. Title 47**, Section 15 of the Code of Federal Regulations, SubPart F: Ultra-wideband.[Online].Available:http://www.access.gpo.gov/nara/cfr/wais idx_05/47cfr15_05.html

[64] **Application Note 150-2**. Spectrum Analysis…Pulsed RF, Agilent Spectrum Analyzer Series, Agilnet Technologies.

[65] **IEEE standard definitions of terms for antennas**., 21 June 1993: IEEE Std.

[66] **E.K. Miller and J.A. Landt,** November 1980: Direct Time-Domain Techniques for Transient Radiation and Scattering from Wires. Proceedings IEEE, Vol. 68, No. 11, pp. 1396–1423.

[67] **C. A. Balanis**, 2005: Antenna Theory. Analysis and Design., Third ed. Wiley-Interscience.

[68] **H. Schantz**, 2005: The Art and Science of Ultrawideband Antennas. Artech House.

[69] **P.-S. Kildal**, 2000: P.-S. Kildal, Foundations of antennas. A unified approach, Textbook coming with the interactive electronic handbook Antenna Design using Mathcad, Studentlitteratur, Lund, Sweden. www.studentlitteratur.se_antennas.

[70] **IEEE standard definitions of terms for antennas**., 21 June 1993: IEEE Std.

[71] **G. Smith**, July 1977: An analysis of the wheeler method for measuring the radiating e-ciency of antennas. Antennas and Propagation, IEEE Transactions on, vol. 25, no. 4, pp. 552-556.

[72] **D. Pozar and B. Kaufman**, January 1988: Comparison of three methods for the measurement of printed antenna efficiency. Antennas and Propagation, IEEE Transactions on, vol. 36, no. 1, pp. 136-139.

[73] **H. Choo, R. Rogers, and H. Ling**, July 2005: On the wheeler cap measurement of the e-ciency of microstrip antennas. Antennas and Propagation, IEEE Transactions on, vol. 53, no. 7, pp. 2328-2332.

[74] **H. Wheeler**, August 1959: The radiansphere around a small antenna. Proceedings of the IRE, vol. 47, no. 8, pp. 1325-1331.

[75] **D. Lamensdorf and L. Susman**, September 1971: An analysis of some directive antennas using time domain measurements. In Proc. Antennas and Propagation Society International Symposium, vol. 9, , pp. 307-310.

[76] **P. Miskovsky, J. Gonzalez-Arbesu, and J. Romeu**, 2009: Antenna radiation e-ciency measurement in an ultrawide frequency range. Antennas and Wireless Propagation Letters, IEEE, vol. 8, pp. 72 -75.

[77] **H. Schantz**, 2002: Radiation effciency of UWB antennas. pp. 351-355.

[78] **R. Johnston**, 2009: E-ciency simulations on a vivaldi antenna in a wheeler cap. In Antennas and Propagation Society International Symposium, APSURSI '09. IEEE, 1-5, pp. 1-4.

[79] **A. Khaleghi**, March 2009: Time-domain measurement of antenna e-ciency in reverberation chamber. Antennas and Propagation, IEEE Transactions on, vol. 57, no. 3, pp. 817-821.

[80] **G. Le Fur, P. Besnier, and A. Sharaiha**, March 2009: E-ciency measurement of UWB antennas using time reversal in reverberation chambers. Electronics Letters, vol. 44, no. 17, pp. 1002-1003, 14.

[81] **X. Zhu, Y. Li, S. Yong, and Z. Zhuang**, January 2009: A novel denition and measurement method of group delay and its application. IEEE Trans. Instrum. Meas., vol. 58, no. 1, pp. 229-233.

[82] Understanding the Fundamental Principles of Vector Network Analysis, Application note 1287-1 ed., Agilnet Technologies, 2005.

[83] **O. Ostwald**, July 1997: Group and Phase Delay Measurements with Vector Network Analyzer ZVR, application note 1ez35_1e ed., Rohde & Schwarz, Munich, Germany.

[84] CST Microwave Studio 2009: [Online]. Available: http://www.cst.com/Content/Products/MWS/Overview.aspx

[85] Ansoft High Frequency Structure Simulator (HFSS) v12.0, 2009: [Online]. Available: http://www.ansoft.com/products/hf/hfss/

[86] **A. Pintado Rodríguez**, 2008: Ultrawideband antenna characterization. Master's thesis, Ecole Polytechnique Fédérale de Lausanne.

[87] HFSS User guide fullbook, http://www.ansys.com/Products/Simulation+Technology/Electronics/ Signal+Integrity/ANSYS+HFSS

CURRICULUM VITAE

Name, Surname	:	Vala TASHVIGH
Place and date of birth	:	OROUMIEH - 21/03/1986
Permanent Address	:	Daneshkadeh intersection, HOFMANN Profile Branch, OROUMIEH, IRAN
E-Mail	:	v.tashvigh@gmail.com
B.Sc.	:	Electrical and Electronics Engineering, Tabriz Azad University